

HETEROCYCLES, Vol. 87, No. 6, 2013, pp. 1209 - 1240. © 2013 The Japan Institute of Heterocyclic Chemistry
Received, 11th April, 2013, Accepted, 26th April, 2013, Published online, 14th May, 2013
DOI: 10.3987/REV-13-769

SYNTHESIS AND CHARACTERIZATION OF TRIPHRYRINS: A NEW FAMILY OF PORPHYRINOIDS

Daiki Kuzuhara¹ and Hiroko Yamada^{1,2*}

¹Graduate School of Materials Science, Nara Institute of Science and Technology, Ikoma 630-0192, Japan, hyamada@ms.naist.jp; ²CREST, JST, Ikoma 630-0192, Japan

Abstract –This article reviews the recent reports about the syntheses, structures, photophysical and redox properties of newly synthesized [14]triphyrins(2.1.1), their metal complexes and their core-modified triphyrins, following the overview of the other triphyrin relatives containing three pyrrole rings and more than three methine carbons. Free-base [14]triphyrins(2.1.1) work as tridentate monovalent anionic cyclic ligands and a variety of metal complexes with Re(I), Mn(I), Ru(II), Pd(II), Pd(IV), Fe(II), Fe(III) and B(III) ions were obtained due to the flexible structure of the triphyrin macrocycles. The core-modified [14]triphyrin(2.1.1) was also expected, but the alkoxy-substituted compounds were obtained instead of the desired thiatriphyrin, probably because of the larger size of sulfur atom compared to nitrogen atom and the electronic repulsion between the lone pairs of inner nitrogen atoms.

CONTENTS

1. Introduction
 - 1-1 Corroles and [14]triphyrins(1.1.1)
2. Synthesis and properties of ring-contracted porphyrins and their metal complexes
 - 2-1 Subpyriporphyrins
 - 2-2 [18]Triphyrins(6.1.1)
 - 2-3 [18]Triphyrins(4.1.1)
 - 2-4 [15]Triphyrins(3.1.1)
3. Synthesis and characterization of free-base [14]triphyrins(2.1.1)
 - 3-1 Synthesis and statistic properties
 - 3-2 Spectroscopic properties
4. Synthesis and characterization of metal complexes of [14]triphyrins(2.1.1)

- 4-1 Octahedral coordinated manganese(I), rhenium(I) and ruthenium(II) complexes
- 4-2 Platinum(II) and platinum(IV) complexes
- 4-3 Iron(II) and iron(III) complexes
- 4-4 Tetrahedral coordinated boron(III) complexes
- 5. Core-modified triphyrins
 - 5-1 Thiatriphyrin(2.1.1) derivatives
- 6. Conclusion

1. INTRODUCTION

1-1 CORROLES AND [14]TRIPHyrINS(1.1.1)

Ring-contracted porphyrins are a series of porphyrinoids, which lack *meso*-carbon atoms or one of four pyrroles. Corroles lack one methine carbon from porphyrins and have one direct pyrrole-pyrrole link (Figure 1).¹ They are known as important ligands that stabilize high valence metal ions. In addition, norcorrole has been reported to lack two methine carbons from the parent porphyrin (Figure 1). Norcorroles have two direct pyrrole-pyrrole links and the nickel complex showed the smallest antiaromatic character with 16 π -electrons.²

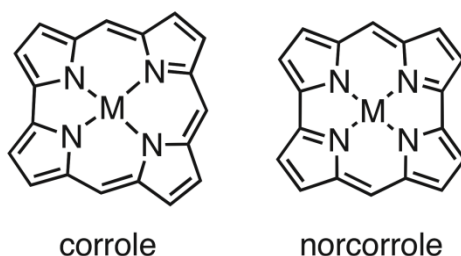


Figure 1. Structures of corrole and norcorrole

On the other hands, triphyrin is a subclass of modified porphyrins described by a general formula $[N]$ triphyrin($x.y.z$) (N = sum of macrocyclic π -electrons; $x, y, z \geq 1$: numbers of linker atoms between pyrroles) and consists of only three pyrrole or pyrrole related heterocycles. There have been a lot of reports about ring-expanded porphyrinoids³ to date, but the chemistry of the ring-contracted porphyrinoids is relatively new. First triphyrin-related compound was subphthalocyanine reported in 1972,⁴ then the next relative, subporphyrazine, was only reported in 2005.⁵

In 2006 Osuka *et al.* reported the synthesis of tribenzosubporphyrins ([14]benzotriphyrins(1.1.1)).⁶ Subsequently, Kobayashi, Osuka, and co-workers independently developed synthetic protocols for *meso*-aryl substituted subporphyrins.^{7,8} Interestingly subphthalocyanines and subporphyrins have a boron

atom in the cavity of the divalent-tridentate cyclic structures with a monoanionic axial ligand. The X-ray single crystal analysis gave the bowl-shaped structure and the boron atom could never be removed. Only recently a planar-shaped subporphyrin borenium cation was obtained as a carborane anion salt.⁹ In contrast to the porphyrins and phthalocyanines, the electronic structure of these molecules is based on a 14π -electron system, since there are three, rather than four, pyrrole or isoindoline moieties. These subporphyrins have strong fluorescence properties and the emission can be tuned by the *meso*-substituents effectively. In recent years considerable interest has appeared in subphthalocyanines and subporphyrins due to the potential applications in a variety of high technology fields as non-linear optical absorption, highly fluorescent compounds, organic light emitting diodes (OLED) and organic solar cells (OSC). Several good reviews about [14]triphyrins(1.1.1) (subporphyrins and subphthalocyanines) have been already published.¹⁰ Therefore, recent progress of chemistry about subpyriporphyrins, [18]triphyrins and [14]triphyrins(2.1.1) will be focused in this review.

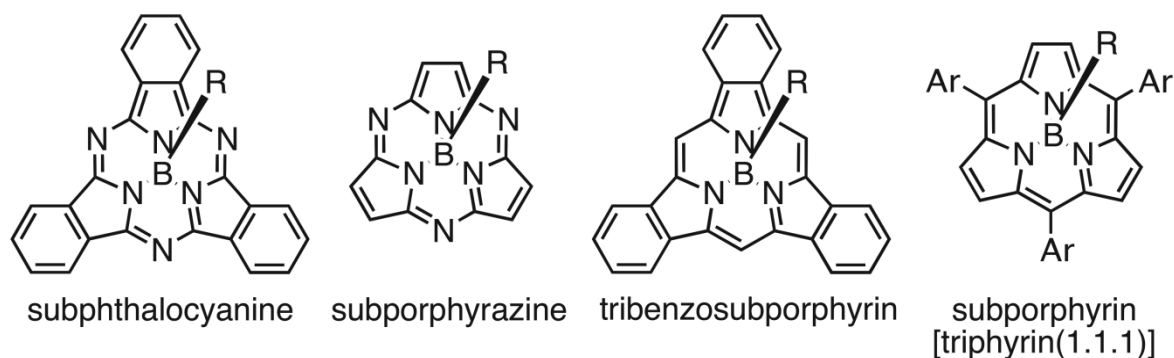
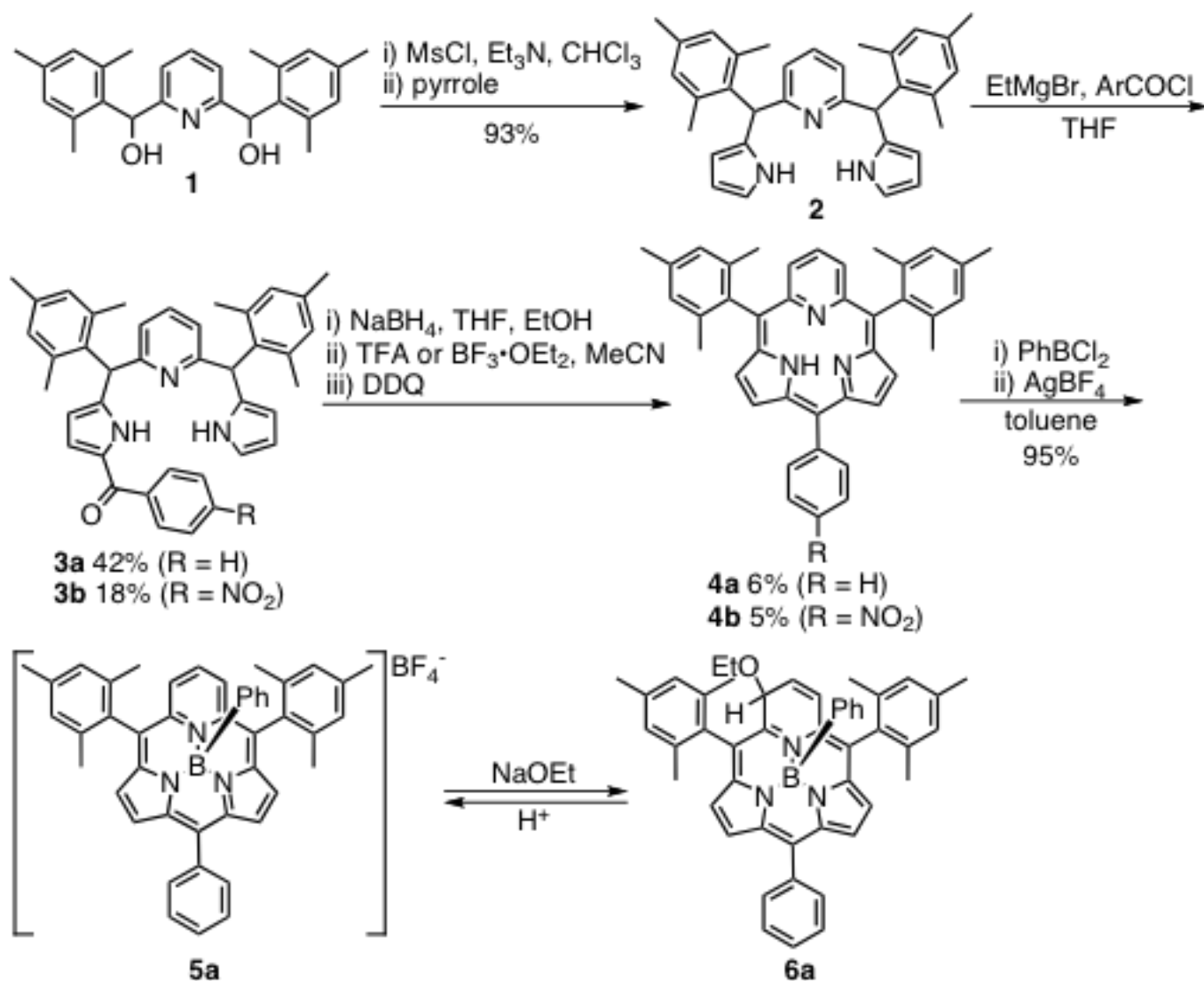


Figure 2. Structures of subphthalocyanine, subporphyrazine, tribenzosubporphyrin and subporphyrin (R = alkoxy, phenoxy, halogen and aryl groups)

2. SYNTHESIS AND PROPERTIES OF RING-CONTRACTED PORPHYRINS AND THEIR METAL COMPLEXES

2-1 SUBPYRIPORPHYRINS

In 2006, subpyriporphyrin was reported as a free-base triphyrin homologue.¹¹ It had one pyridine ring instead of one of three pyrrole rings and showed a non-aromatic electronic structure at free-base form. The synthetic route of subpyriporphyrins is shown in Scheme 1. Pyridine-included tripyrrane **2** was prepared from 2,6-bis[hydroxy-(mesityl)-methyl]pyridine **1** in 38% yield. Monobenzoylation of **2** afforded **3a** (R = H) in 42% yield. Subsequently, reduction of **3a** with NaBH₄ gave alcohol derivative, followed by intramolecular condensation reaction to produce subpyriporphyrin **4a** in 6% yield as green solids. The 11-*p*-nitrophenyl-substituted subpyriporphyrin **4b** was also reported from the same synthetic route (Scheme 1).¹²



Scheme 1. Synthetic route to subpyriporphyrins and their boron complexes

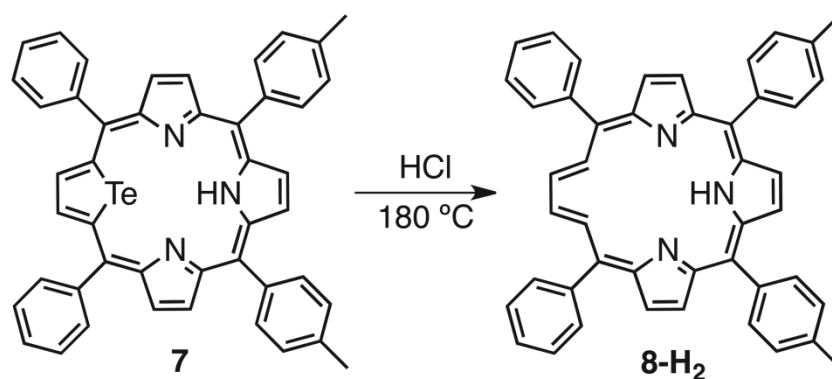
The ¹H NMR spectrum of **4a** showed the extreme downfield shift of NH resonance (18.07 ppm in CD₂Cl₂, 203 K) resulted from the strong hydrogen bonding interaction. The X-ray crystal structure of **4a** showed the slightly ruffled structure. The inner proton laid in three-centered strong hydrogen bonding with N-N distances of 2.370(2) and 2.534(2) Å. The peripheral substituent could be changed from phenyl group to *p*-nitrophenyl group, then the absorption spectrum arising from charge-transfer (CT) transition was observed.¹² Furthermore, the NH-tautomerization was a key factor determining the excited state dynamics: at 293 K the fluorescence lifetime was 8 ps due to the excited state proton transfer from pyrrole-nitrogen to pyridine-nitrogen, but at 77 K in 2-methyltetrahydrofuran, below its melting-point, the tautomerization was locked and the excited state lifetime was long as 458 ps.

The reaction of subpyriporphyrin **4a** with PhBCl₂ gave dome shaped σ-phenyl boron (III) triphyrin complex **5a**, wherein the macrocycle acted as a monoanionic tridentate ligand.¹¹ The ¹H NMR resonances of the boron complex showed marked downfield shifts in comparison with those of subpyriporphyrin **4a**

and the signal of *ortho*-protons of B-phenyl was observed at 4.87 ppm, revealing a significant contribution by the ring current. When ethoxide ion was added to the boron complex, ethoxide was inserted to the *m*-position of pyridine moiety as a mixture of two aromatic stereoisomers.

2-2 [18]TRIPHYRINS(6.1.1)

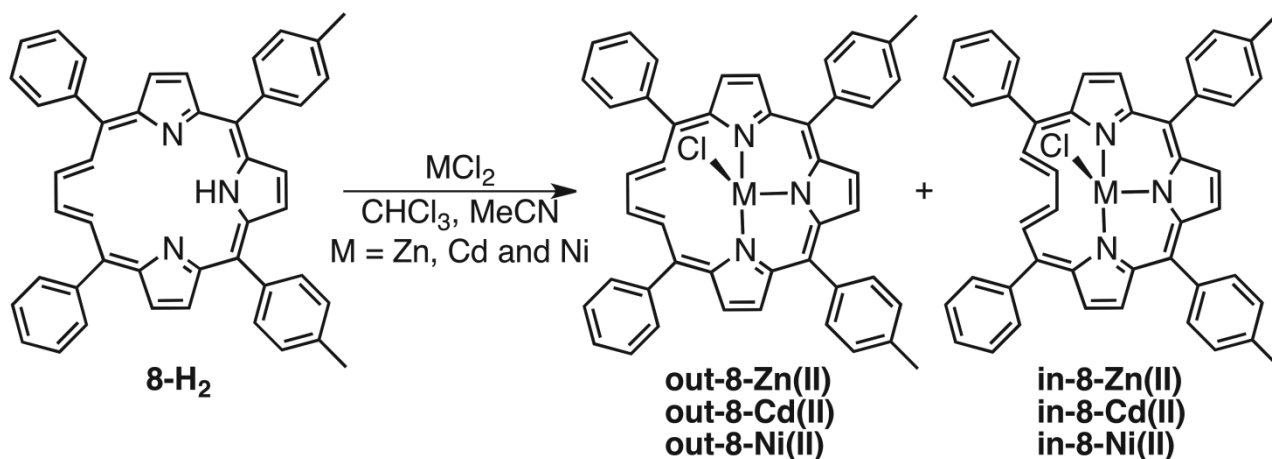
In 2002, Latos-Grażyński *et al.* have reported 21-vacataporphyrin (**8-H₂**; [18]triphyrin(6.1.1)), which was prepared by acid treatment of telluraporphyrin **7** to remove Te atom (Scheme 2).¹³ It has a butadiene linker due to a lack of the nitrogen atom from the parent porphyrin. The signals of butadiene parts were observed at -2.50 ppm (inside) and 9.65 ppm (outside), which clearly showed the nature of the 18 π -electron macrocyclic aromaticity. The free-base compound **8-H₂** showed nearly flat structure from X-ray single crystal diffraction and the spectroscopic and structural features are similar to the parent porphyrin.



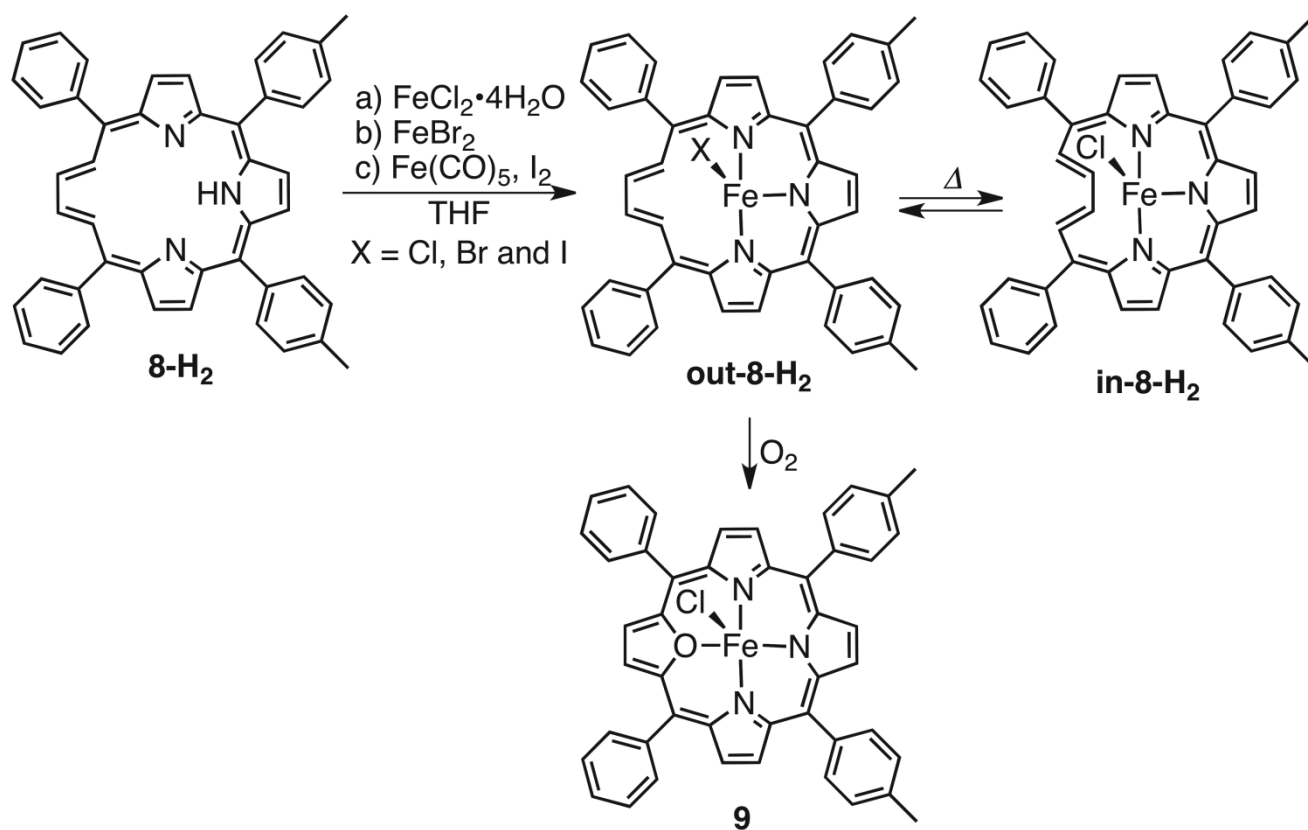
Scheme 2. Synthesis of 21-vacataporphyrin **8-H₂** ([18]triphyrin(6.1.1))

This macrocycle **8-H₂** is a monovalent anionic ligand. The diamagnetic **8-Zn(II)** and **8-Cd(II)** complexes and a paramagnetic **8-Ni(II)** complex have been reported, coordinated to three pyrrolic nitrogens.¹⁴ Coordination imposes a steric constraint on the ligand geometry and leads to stereoisomers with the annulene part oriented outward-**8-M(II)** (**out-8-M(II)**) or inward-**8-M(II)** (**in-8-M(II)**) (M = Zn, Cd and Ni) macrocyclic center (Scheme 3). The **out-8-Zn(II)**, **out-8-Cd(II)** and the free-base **8-H₂** share a common ¹H NMR spectral pattern as the basic structural features, which are preserved after the metal ion insertion. The ¹H NMR spectra of **in-8-Zn(II)** and **in-8-Cd(II)** reflect a considerable decrease of aromaticity accounted by the inverted geometry.

The **8-Fe(II)** also showed the isomers at annulene part; the annulene chain oriented inward and outward geometry (Scheme 4).¹⁵ The **out-8-Fe(II)** is more reactive with molecular oxygen than another complex, and gave iron(II) 21-oxaporphyrin complex **9**. All these complexes showed characteristics typical for high-spin iron(II) complexes of porphyrinoids.

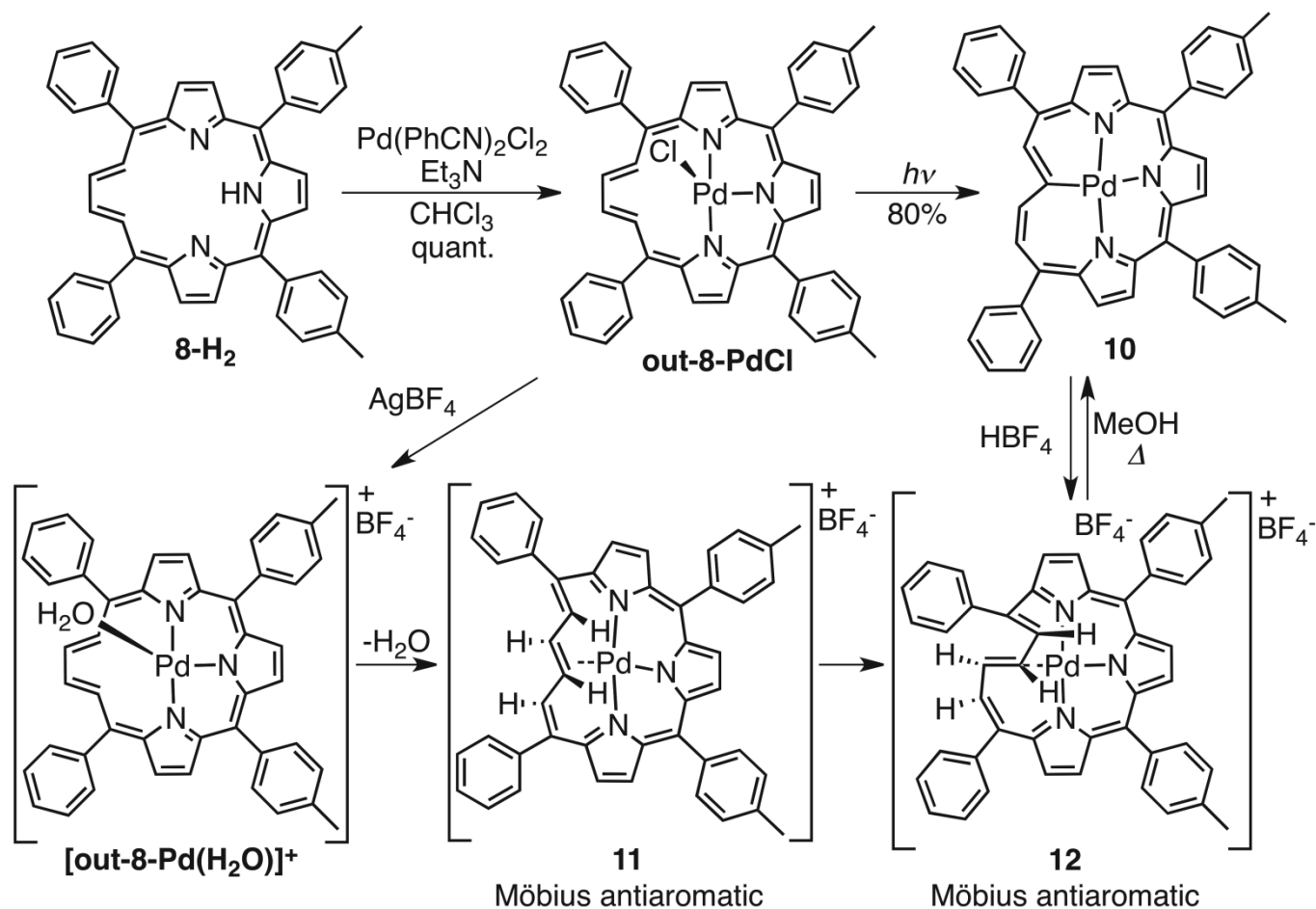


Scheme 3. Synthesis of **out-8-M(II)** and **in-8-M(II)**



Scheme 4. Synthesis of iron(II) vacatoporphyrin complexes

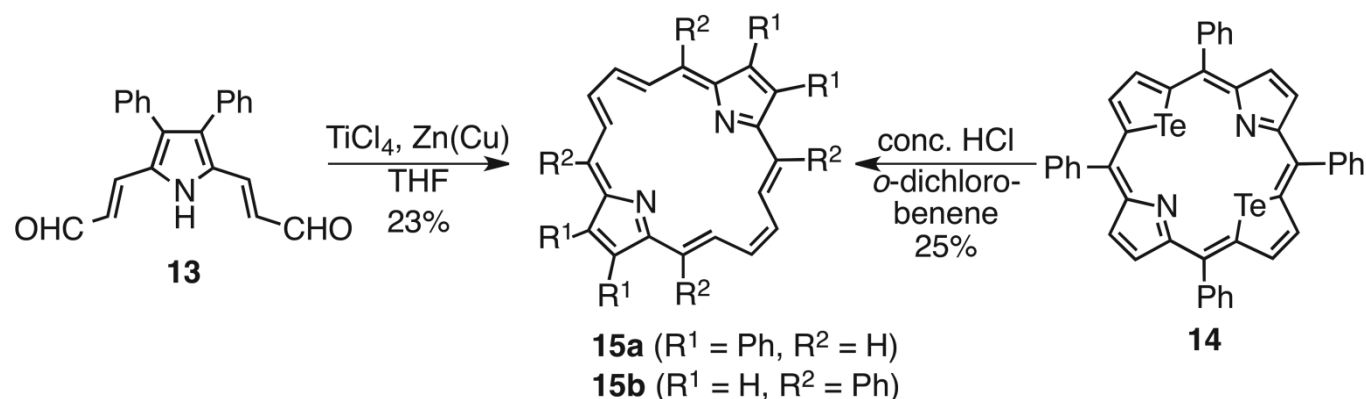
Palladium(II) complexes of the 21-vacatoporphyrin (**out-8-PdCl**) were also prepared (Scheme 5).¹⁶ The **out-8-PdCl** was photochemically changed to the complex **10** having Pd-C bond with leaving of an HCl molecule. The macrocycle revealed the unique structural flexibility triggered by coordination of palladium. The palladium vacatoporphyrin complexes reveal Hückel aromaticity (**out-8-PdCl**, [**out-8-Pd(H₂O**)]⁺ and **10**) or Möbius antiaromaticity (**11** and **12**) of [18]annulene applying the butadiene fragment as a topology selector.



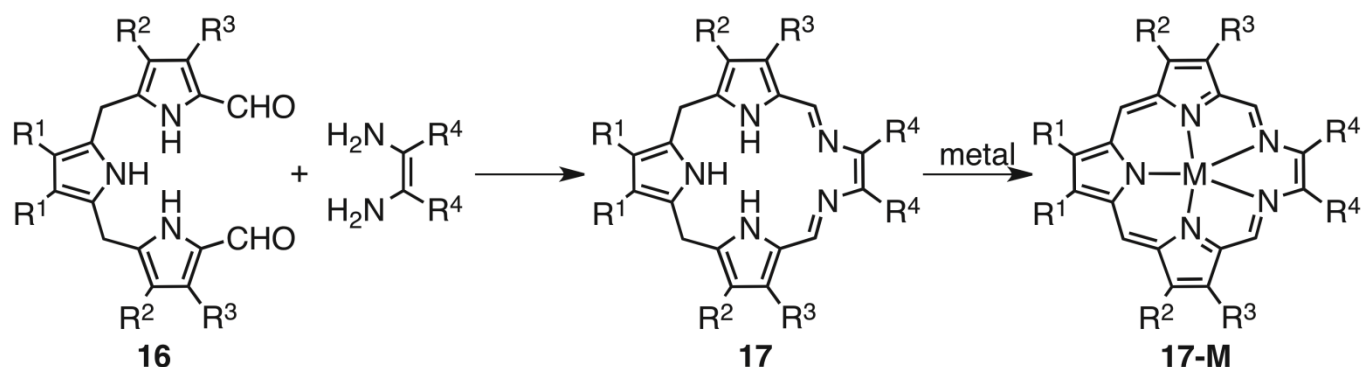
Scheme 5. Synthesis and reactivity of palladium(II) vacataporphyrin complexes

In this regards, divacataporphyrin (dideazaporphyrin) was independently reported by Lash and Latos-Grażyński and their co-workers.^{17,18} Lash *et al.* reported intermolecular McMurry coupling of dialdehyde **13** to give tetraphenyl dideazaporphyrin **15a** in 23% yield. Latos-Grażyński *et al.* reported the synthesis of *meso*-tetraaryldivacataporphyrin **15b** by heating ditelluraporphyrin **14** with concentrated HCl in *o*-dichlorobenzene (Scheme 6). This shows fundamental structural and spectroscopic features of the parent porphyrin, but the framework is flexible. 21-Vacataporphyrin and divacataporphyrin have been investigated in the field of photodynamic therapy (PDT).¹⁹

Texaphyrin was prepared by a Schiff-base derived macrocycle by Sessler *et al.*²⁰ Diformyltripyrane **16** was reacted with ethylenediamine or *o*-phenylenediamine derivatives to afford the hydrotexaphyrins **17**. It lacks a pyrrolic nitrogen atom from the parent porphyrin and replaces two carbon atoms to nitrogen atoms. These macrocycles behaved as mono-anionic pentadentate structures that lead to various metal complexes **17-M** (Scheme 7). In particular, lanthanide ions could be coordinated to texaphyrin and these lanthanide metal complexes were used for biomolecule imaging and PDT. There are several satisfactory reviews and books about texaphyrins and their metal complexes.^{21,22}



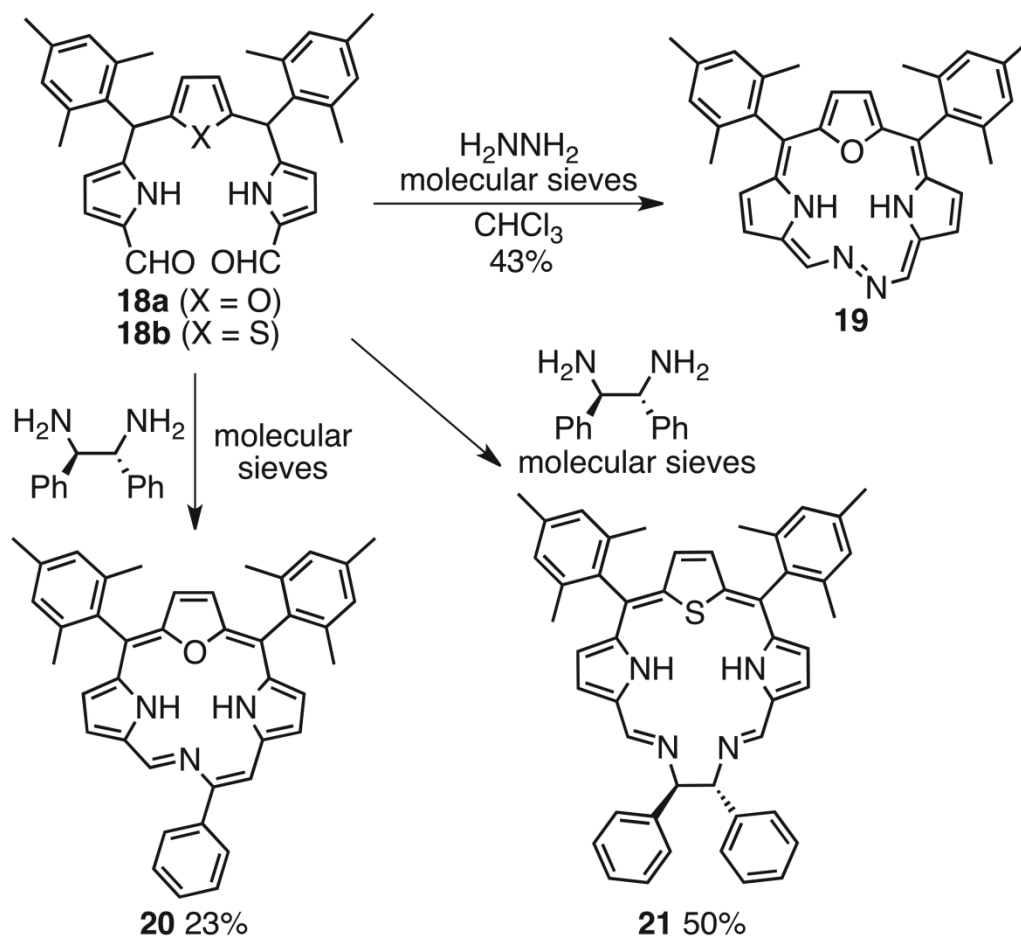
Scheme 6. Synthesis of divacataporphyrins **15** (21,23-dideazaporphyrins)



Scheme 7. Synthesis and metal complexes of texaphyrins **17**

2-3 [18]TRIPHYRINS(4.1.1)

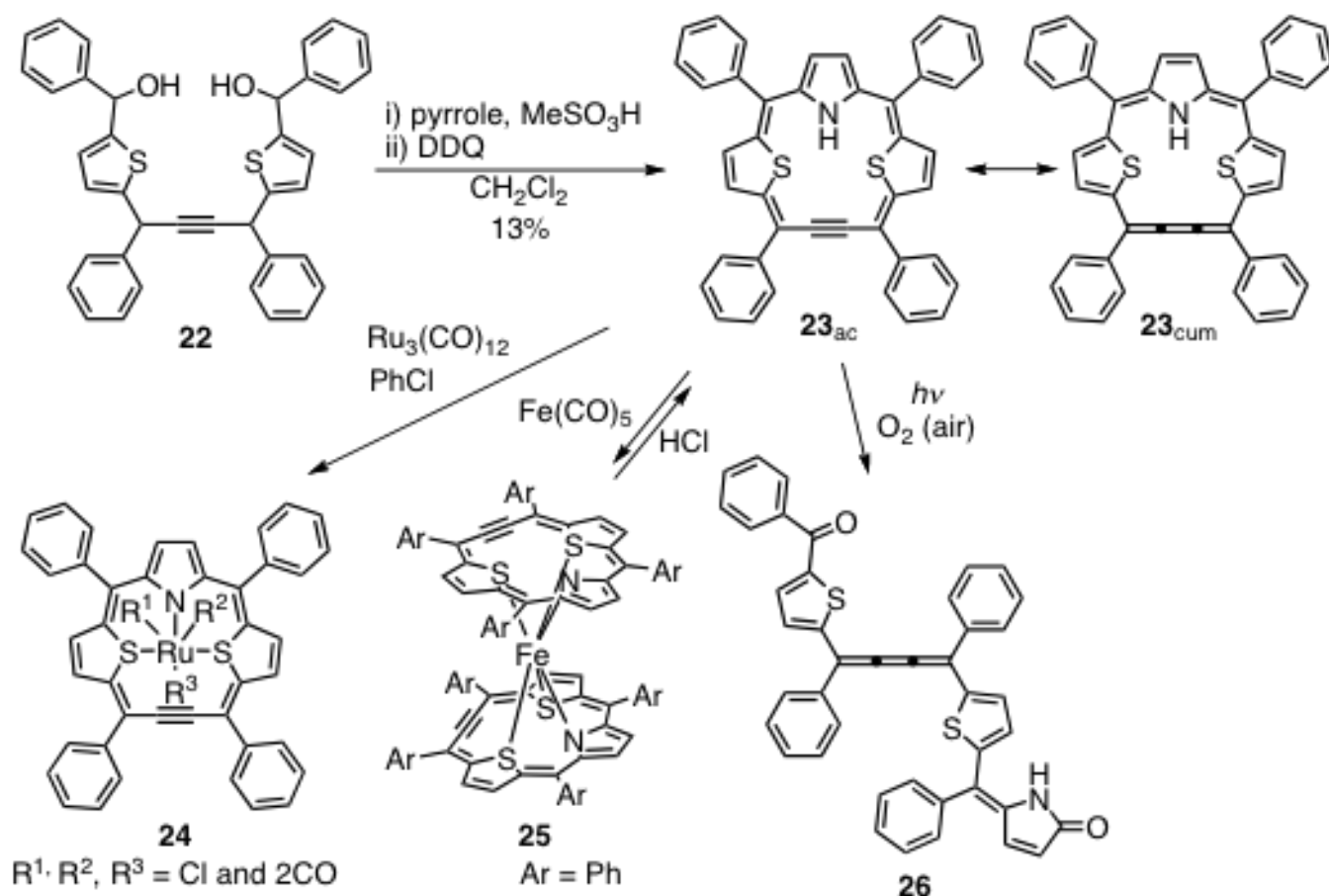
In 1999, Lee *et al.* reported Schiff-base derived [18]oxatriphyrin(4.1.1) derivatives.²³ These macrocycles were synthesized from diformylheterotripyrranes with diamine compounds (Scheme 8). In the case of diformyloxatripyrrane **18a**, it reacted with hydrazine to afford the azo-bridged macrocycle **19** in 43% yield.²³ In addition, a reaction of **18a** and 1,2-diphenyl-ethylenediamine caused the unusual rearrangement to afford the [18]oxatriphyrin(4.1.1) **20** in 23% yield,²³ while diformylthiatripyrrane **18b** and 1,2-diphenyl-ethylenediamine gave only macrocycle **21** which was formed by a general addition-elimination reaction of aldehyde and amine.²⁴ From ¹H NMR spectra, the N-H protons of **20** were observed at -1.38 and -0.84 ppm. This result indicated clear evidence of macrocyclic aromaticity. The absorption spectrum of **20** showed Soret-like band at 381 nm and five less-intense bands at 436, 461, 489, 554 and 603 nm, similar absorption shape with corroles, indicating [18]oxatriphyrin(4.1.1) **20** has the corrole-like macrocyclic aromatic characters. In contrast, NH-protons of macrocycle **21** were observed at 9.89 ppm and 8.08 ppm at 223 K, which were the chemical shifts of normal pyrrolic hydrogen.



Scheme 8. Synthesis of [18]triphyrins(4.1.1) derivatives

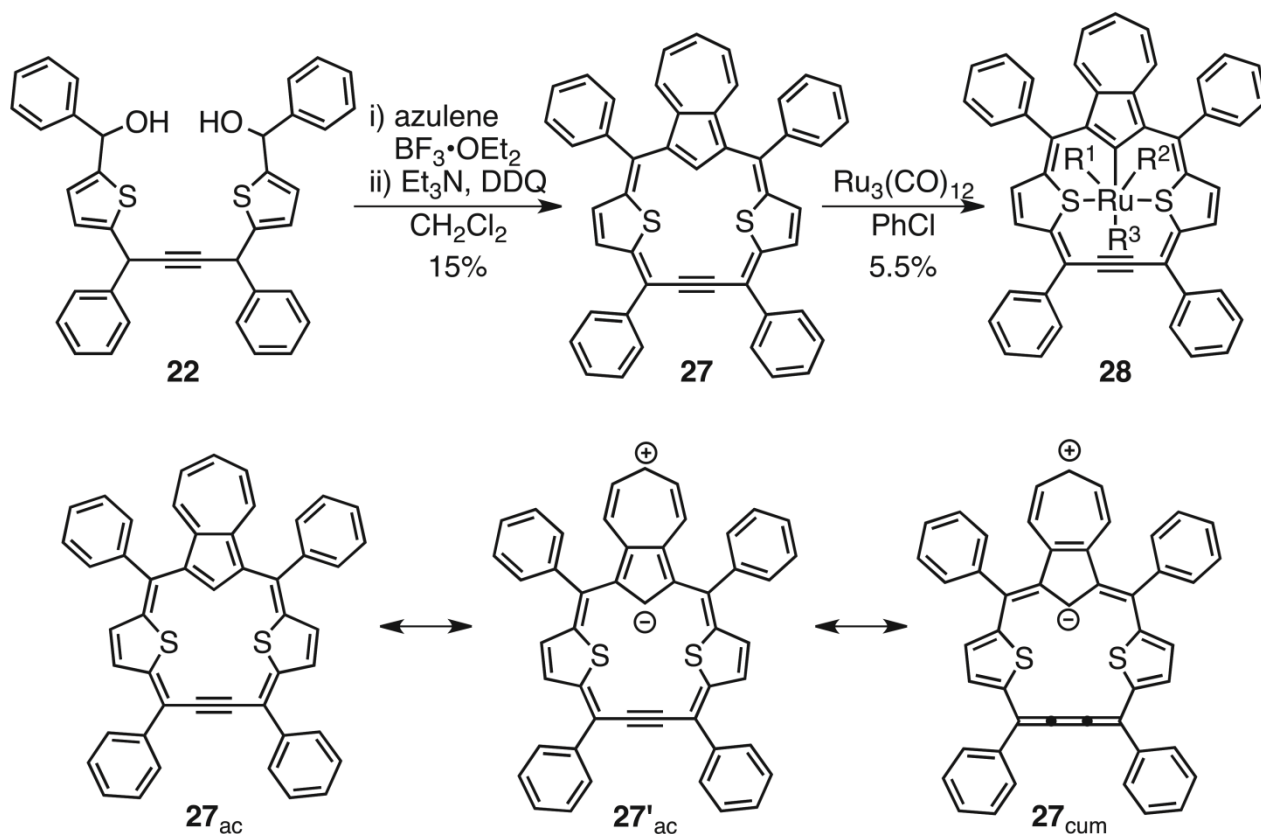
Then Latos-Grażyński *et al.* have reported core-modified [18]triphyrin(4.1.1) compounds (Scheme 9). These compounds include one ethynyl bond at *meso*-position and one or two thiophene rings instead of pyrrole rings. Dithiaethyneporphyrin **23** has two thiophene rings and one pyrrole ring with monovalent property.²⁵ Dithiaethyneporphyrin **23** was obtained from 1,4-bis(4-(phenylhydroxymethyl)thien-2-yl)-1,4-diphenyl-2-butyne **22** and pyrrole in the presence of methanesulfonic acid by [3+1] condensation method in 13% yield. NH proton was observed at -3.24 ppm to show the macrocyclic ring-current effect. Two canonical electronic structures **23_{ac}** and **23_{cum}** can be described as reflecting the combination of acetylene and cumulene character from ¹³C NMR chemical shifts. X-Ray single crystal analysis showed the bow-like deformation at the butyne moiety with C-C bond lengths of 1.390(9), 1.231(19), and 1.418(10) Å, respectively. It could make Ru(II) complex **24** with one Cl⁻ and two CO ligands. Due to the lower symmetry of ¹H NMR spectrum, octahedral coordination of dithiaethyneporphyrin with severely tilted two thiophene rings to opposite side was considered. Double-decker Fe(II) complex **25** was also reported.²⁶ This was the first example of porphyrin double-decker complex reported for the transition metals of groups 6 to 11. Dithiaethyneporphyrin rings can rotate around the Fe(II) ion. The variable temperature ¹H NMR studies revealed two enantiomeric

couples of four fundamentally staggered rotamers were involved. In the presence of O_2 , dithiaethyneporphyrin **23** showed oxidative cleavage to open-chain diastereomer **26** terminated by carbonyl groups.²⁷



Scheme 9. Synthesis and canonical structures of dithiaethyneporphyrin **23** and its metal complexes

Dithiaethyneazuliporphyrin **27** has one azulene and two thiophene rings on behalf of three pyrrole rings (Scheme 10).²⁸ It was prepared by Rothmund-type condensation of diol compound **22** and azulene in 15% yield. Three canonical structures defined 18 π -electron macrocyclic delocalization pathways. From ^{13}C NMR, acetylene carbon atoms of **27** were observed at 106.1 ppm, upfield region compared to dithiaethyneporphyrin **23** (116.8 ppm). Thus the acetylene character prevailed in this compound. It could make ruthenium complex **28** as a monoanionic ligand, forming the $Ru-C$ σ -bond at inner carbon of azulene. This complex was C_s symmetry with a mirror plane passing through the ruthenium, chloride, and coordinated azulene carbon.

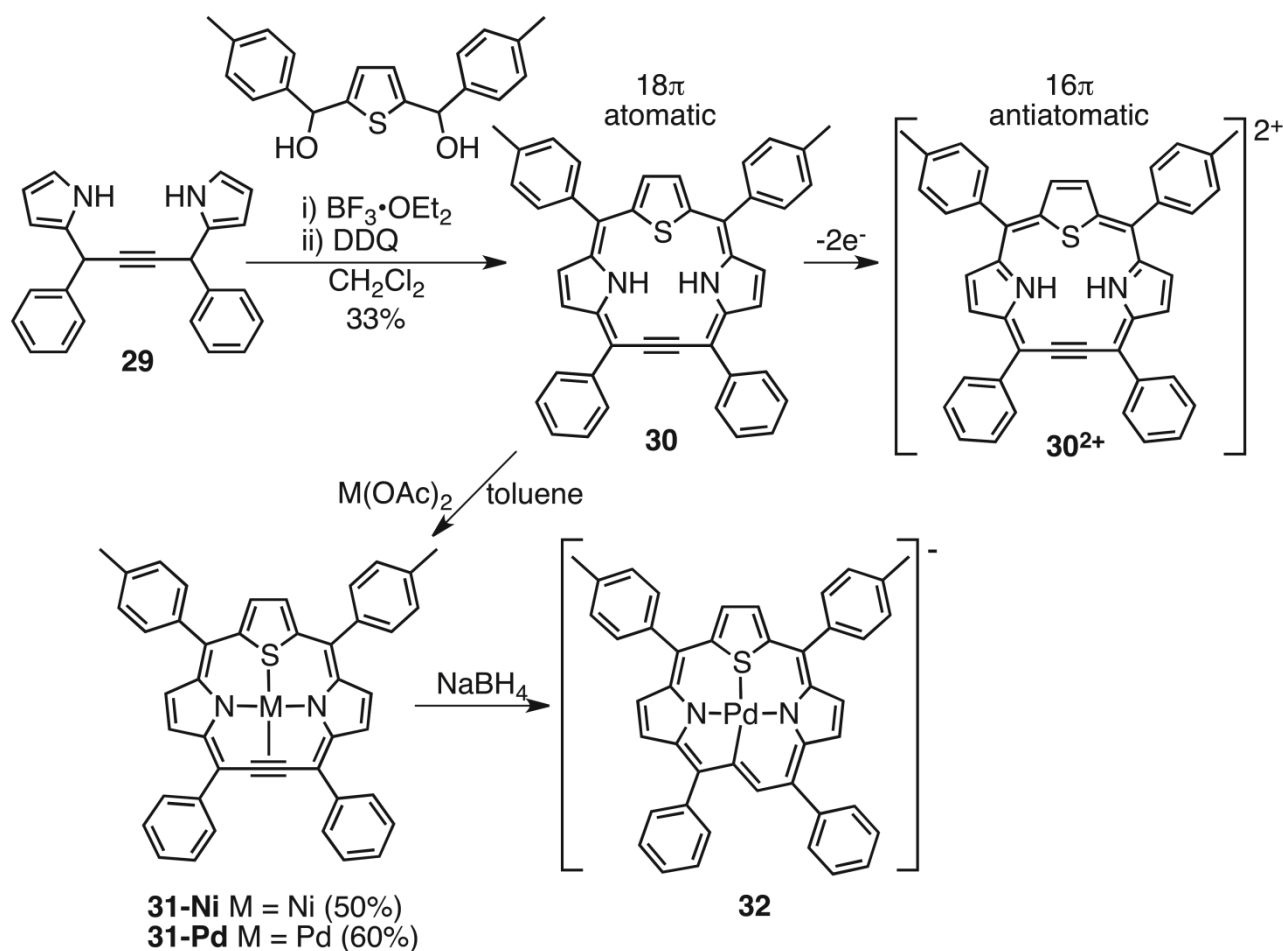


Scheme 10. Synthesis and canonical structures and ruthenium complex of dithiaethyneazuliporphyrin **27**

In 2012 thiaethyneporphyrin **30** with one thiophene and two pyrrole rings was obtained in a simple modification of the [3 + 1] approach described for the synthesis of porphyrins (Scheme 11).²⁹ NH protons at -3.29 ppm and β -pyrrolic hydrogen atoms confirmed the 18π -electron structure. From ^{13}C NMR spectrum, both of the acetylene and cumulene structure contributed to the electronic structure, although the cumulenenic character was predominant. Two-electron oxidation of thiaethyneporphyrin gave 16π -compound **30²⁺** and the NH protons at 25.35 ppm showed the paratropic ring current was present in the macrocycle. Making intramolecular metal(II)- η^2 -CC bond, **31-Pd** and **31-Ni** complexes were obtained. **31-Pd** complex was reduced by NaBH_4 , then $\text{Pd(II)}-\eta^2\text{-C}^1\text{C}^2$ interaction has been replaced by the typical $\text{Pd(II)}-\text{C}$ σ bond ($\text{Pd}-\text{C}^1$), affording the complex **32** of a regular carbaporphyrinoid, which was observed by ^1H NMR measurement. The NaBH_4 treatment of free base thiaethyneporphyrin **30** gave aromatic 20-thiaethyneporphyrin. The NaBH_4 treatment of Ni(II) complex only gave the demetalation. The titration of **31-Ni** with pyridine converted the low-spin species into the high-spin complex due to the axial ligand.

2-4 [15]TRIPHYRINS(3.1.1)

The synthesis of [15]triphyrin(3.1.1) **34** has been reported by Anderson *et al.* (Scheme 12).³⁰ The acid-



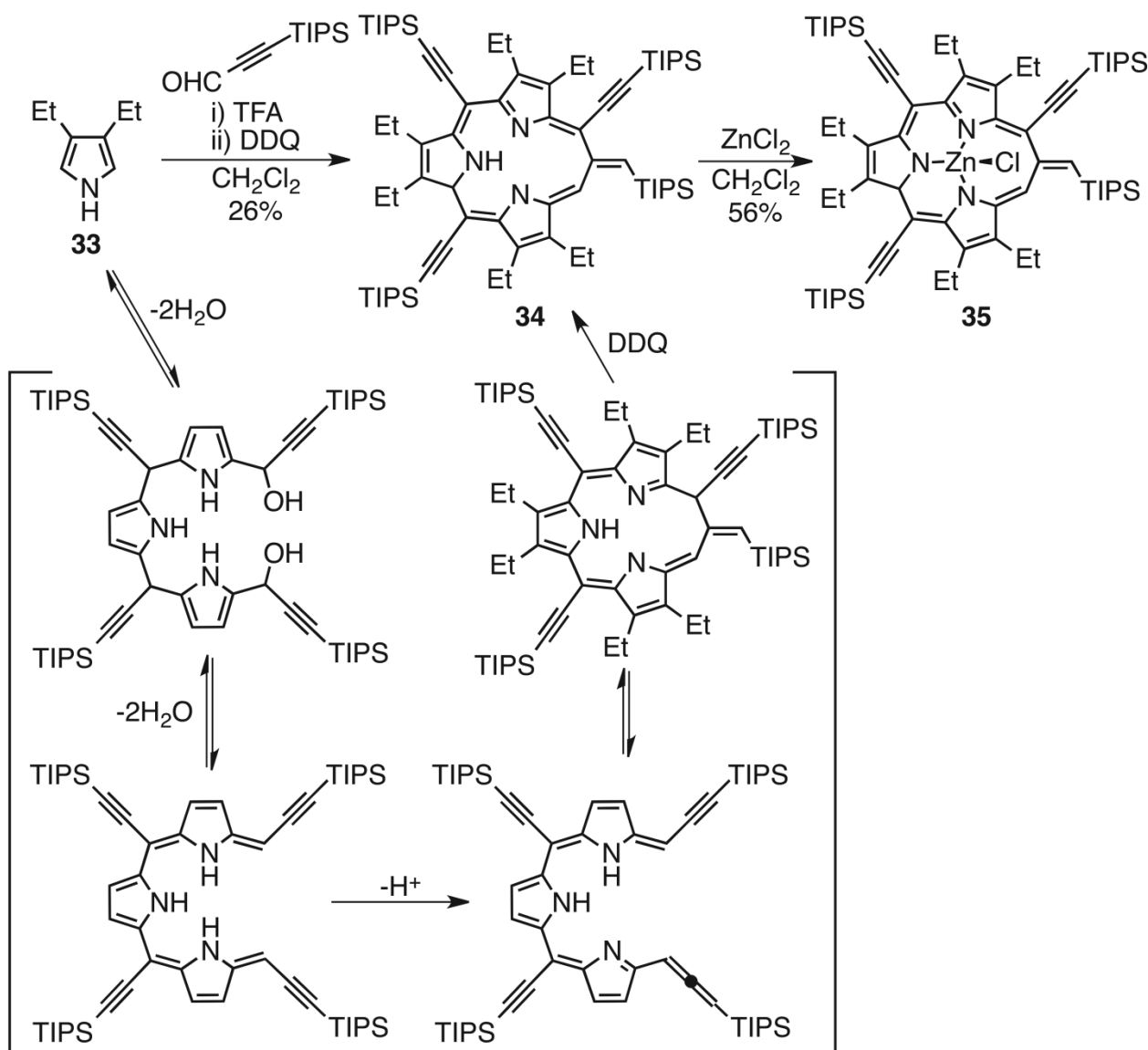
Scheme 11. Synthesis, reactivity and metal complexes of thiaethyneporphyrin **30**

catalyzed Rothemund condensation of TIPS-propynal and diethylpyrrole **33** followed by the oxidation with DDQ gave [15]triphyrin(3.1.1) **34** with corrole, porphyrin, [24]pentaphyrin(1.1.1.1.1), [28]hexaphyrin(1.1.1.1.1.1), and two linear tripyrromethenes. In the $\text{BF}_3\cdot\text{OEt}_2$ catalyzed reaction [15]triphyrin(3.1.1) **34** was obtained in 3.5% as a byproduct, but it became the main product with 26% yield when the reaction was catalyzed with TFA. The reaction mechanism is shown in Scheme 12. From the X-ray crystal structural analysis of Zn complex **35**, Zn and exocyclic $\text{C}=\text{C}$ bond revealed a remarkable interaction as zinc- η^2 -alkene complex.

3. SYNTHESIS AND CHARACTERIZATION OF FREE-BASE [14]TRIPHYRINS(2.1.1)

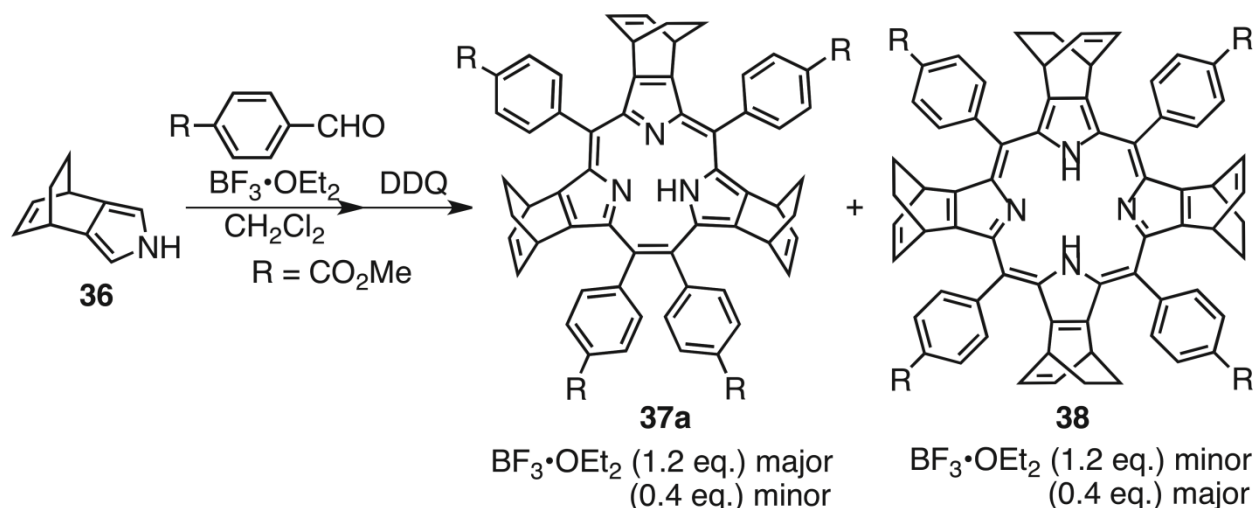
3-1 SYNTHESIS AND STATISTIC PROPERTIES

Recently, [14]triphyrin(2.1.1) **37** has been reported as a new family of free-base 14π -ring contracted porphyrins. The first [14]triphyrin(2.1.1) **37a** was prepared serendipitously by Shen, Yamada, You, and Kobayashi *et al.* in 2008 by a modified Lindsey's method (Scheme 13).³¹ They intended the preparation of *meso*-tetraaryl bicycle[2.2.2]octadiene(BCOD)-fused-porphyrin **38** in the presence of $\text{BF}_3\cdot\text{OEt}_2$ by the



Scheme 12. Synthesis and reaction mechanism of [15]triphyrin(3.1.1) **34** and its zinc complex **35**

previously reported method.³² Then, interestingly, the treatment of an equimolar mixture of BCO_D-fused pyrrole **36** and methyl 4-formylbenzoate with 1.2 eq. of $\text{BF}_3 \cdot \text{OEt}_2$ followed by oxidation with DDQ gave [14]triphyrin(2.1.1) **37a** in 34% yield unexpectedly, while with the normal concentration (0.4 eq.) of $\text{BF}_3 \cdot \text{OEt}_2$ gave tetraarylporphyrin **38** as usual. This [14]triphyrin(2.1.1) **37a** has flat and metal-free structure, which is the first example of metal free ring contracted porphyrinoid with 14π aromaticity. The reaction was monitored by the change of UV-vis spectra. In the presence of 1.2 eq. of acid, typical spectra of triphyrin **37a** (411 nm) and porphyrin **38** (457 nm) were detected 1 h after the acid addition, but gradually the Soret band at 457 nm of porphyrin **38** decreased, and after 12 h only the spectrum of triphyrin **37a** was observed. In the presence of 0.4 eq. of acid, no triphyrin **37a** was observed during the reaction. Therefore the accidental high concentration of acid seems to induce the preparation of [14]triphyrin(2.1.1) **37a**.³³ The [14]triphyrins(2.1.1) **37b-e** were also prepared with 4-fluorophenyl,

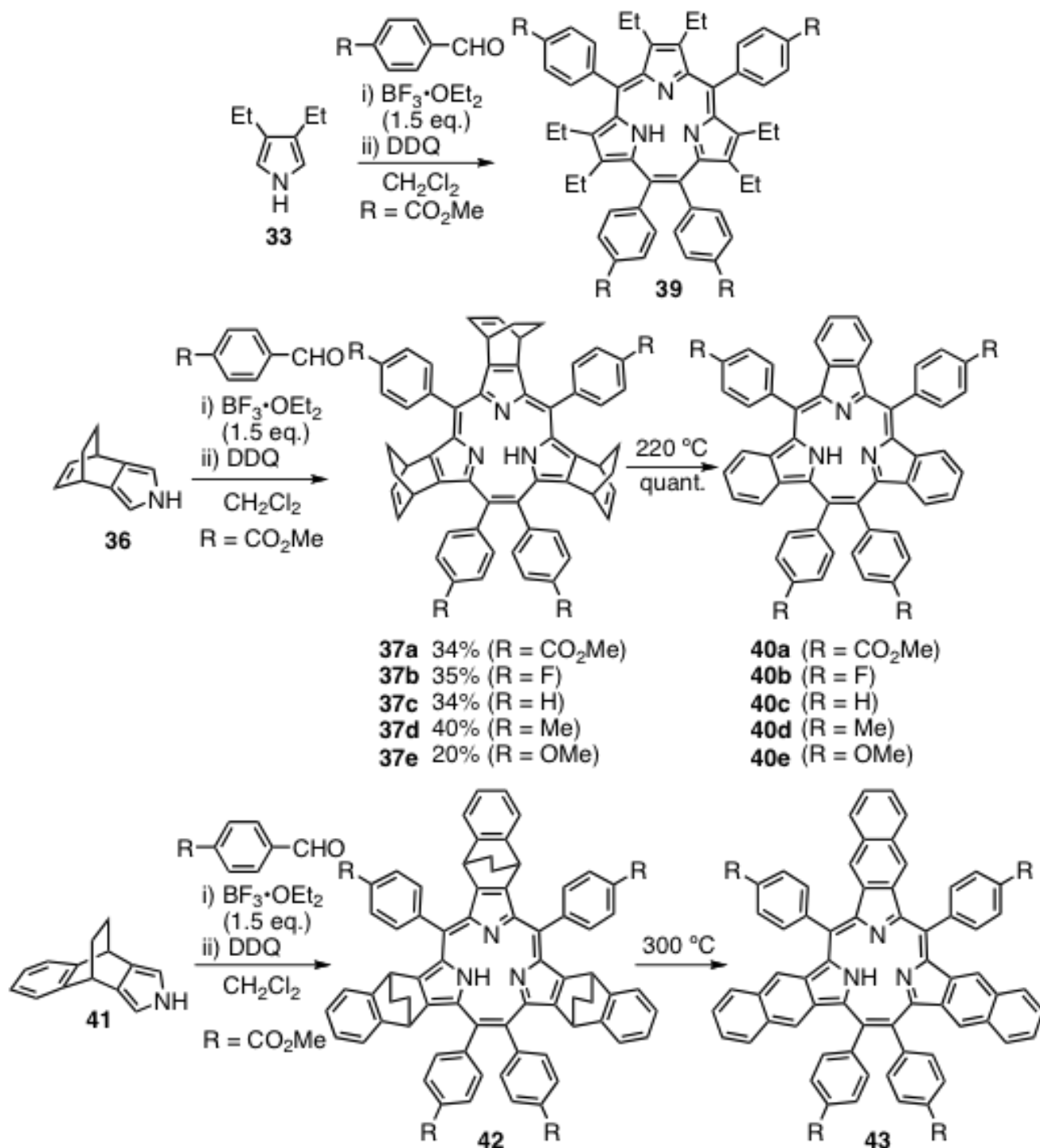


Scheme 13. Synthetic conditions of [14]triphyrin(2.1.1) and porphyrin by Lindsey method

phenyl, 4-tolyl, and 4-methoxybenzaldehyde in 20-40% yields (Scheme 14). The pyrrole moiety was also changeable to 3,4-diethylpyrrole **33** and dihydroethanonaphthalene pyrrole **41** moieties with relatively lower yield. The BCOD framework can be converted to benzo- or naphtho-group by retro-Diels-Alder reaction at 220 °C or 300 °C, respectively.³³ Thus, the Lindsey's method is suitable for the tetraaryl-triphyrins with same substituents at β -positions of pyrroles and *meso*-position, respectively. If pyrroles and arylaldehydes are available, the triphyrins can be obtained only by acid-catalyzed cyclization and oxidation.

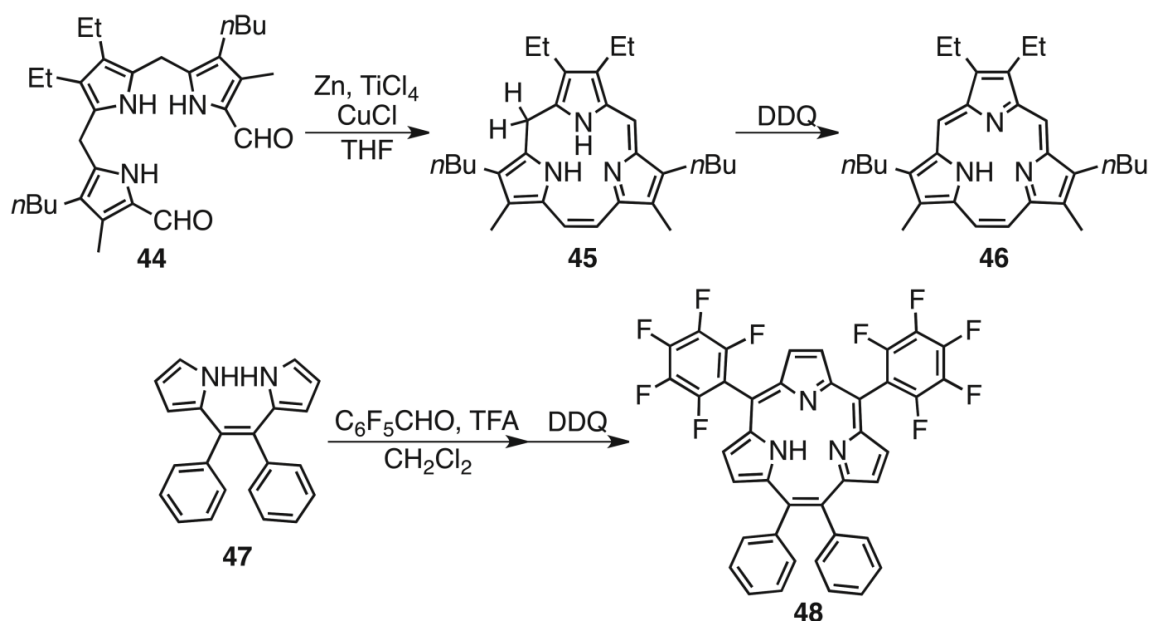
In 2011, we reported *meso*-free-hexaalkyl-triphyrins **46** by an intramolecular McMurry coupling of diformyltripyrane **44** followed by oxidation with DDQ in 16% yield in 2 steps (Scheme 15).³⁴ The intermediate **45** before oxidation was purified and characterized successfully. McMurry coupling needs stepwise synthesis of tripyrranes, but the substituents at β -position can be changed freely. The core-modified triphyrin can be also expected by insertion of heteroaromatic compounds instead of pyrrole. The *meso*-aryl- β -free triphyrin(2.1.1) **48** was reported by Anju *et al.* in 2011, by acid-condensation of 5,6-diphenyldipyrromethane **47** with pentafluorobenzaldehyde, followed by oxidation with DDQ in 5% yield (Scheme 15).³⁵ The mechanism was speculated as the condensation reaction of the starting materials with a free pyrrole obtained in situ, followed by an oxidation. This was the first example of β -free triphyrin(2.1.1) with two kinds of aryl groups at *meso*-positions.

In general ^1H NMR spectra of porphyrin NH protons are observed around 0 to -2 ppm due to the diatropic ring current of the porphyrin macrocycle. On the contrary triphyrins showed unusual downfield shifts of inner NH protons at 7.68 ppm for **37a**, 8.16 ppm for **40a**, 9.0 ppm for **43**, 7.25 ppm for **46** and 9.07 ppm for **48** due to the strong inner hydrogen bonding. Such downfield shift was also observed for porphycenes,³⁶ isocorroles³⁷ and *N*-fused porphyrins³⁸ with modified central cavities containing significantly shorter N•••N distances than conventional porphyrinoids.



Scheme 14. Synthesis of various [14]triphyrins(2.1.1) by modified Lindsey conditions

The crystal structures of **37c**, **40c** and **46** are shown in Figure 3. Different from the known [14]triphyrin(1.1.1) compounds, [14]triphyrins(2.1.1) are planar metal-free macrocycles and can be anionic monodentate cyclic ligands. For each triphyrin, pyrroles are slightly tilted from the plane made by *meso*-carbons. In particular, the angle of pyrrole 2 and the mean plane of four *meso*-carbons is larger than that made by the other two pyrroles and the mean plane. This is due to the stronger hydrogen bonding



Scheme 15. Synthesis of *meso*-free and β -free [14]triphyrins(2.1.1)

between nitrogen atoms of pyrroles 1 and 3 by the planar conformation. The pivot freedom of pyrrole 1 let the [14]triphyrin(2.1.1) coordinate to the various metal ions, as described in section 4-1.

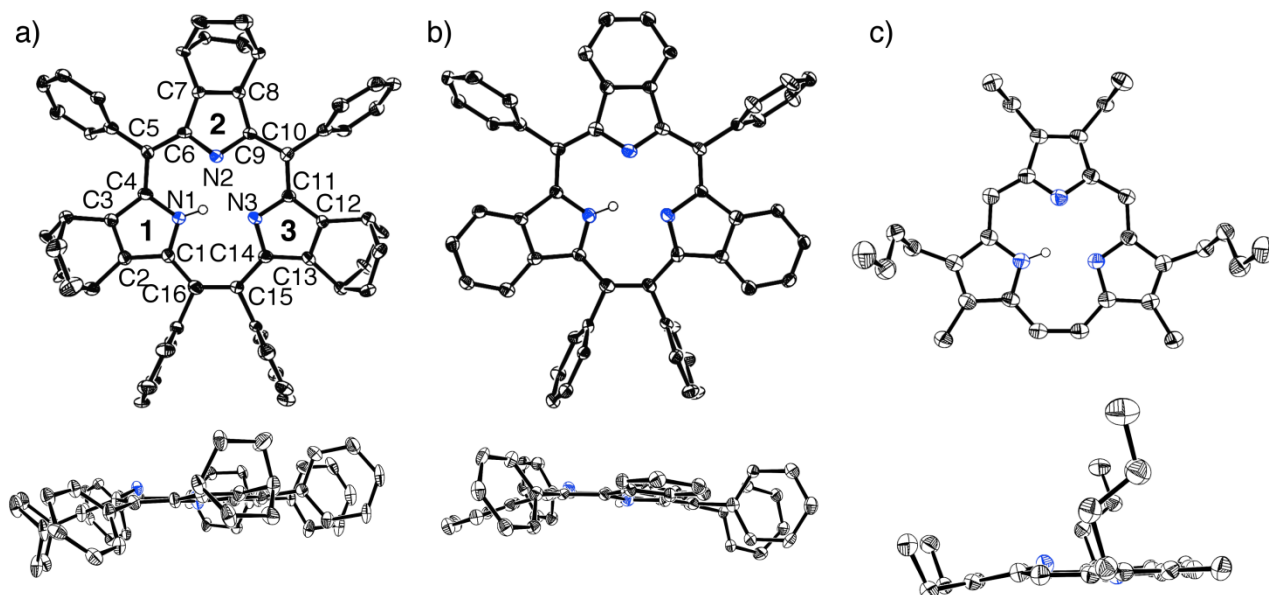


Figure 3. Crystal structures of a) **37c**, b) **40c** and c) **46**. Hydrogen atoms are omitted for clarity except for inner N-H hydrogen atoms. Thermal ellipsoids represent 50% probability.

3-2 SPECTROSCOPIC PROPERTIES

UV-vis absorption spectra of **37c** and **40c** are shown in Figure 4. Triphyrin **37c** showed B-like band at 373 nm and broad Q-like band reached to 600 nm in CH₂Cl₂. With the expansion of π -conjugation, **40c**

showed B-like band at 414 nm and Q-like band at 523 and 578 nm;³¹ **43** showed B-like band at 447 nm and Q-like band at 561 and 614 nm in CH₂Cl₂.³³ The fusion of phenyl rings at β -positions of pyrrole moieties induced the red-shifts of absorption spectra. Triphyrin **46** showed blue-shift compared to the **37c**: B-like band at 336 nm and Q-like band at 440-560 nm with broad peaks at 470 and 550 nm.³⁴ Triphyrins **40c** and **48** were fluorescent at room temperature and the fluorescence quantum yields were 0.018 and 0.008, respectively.^{33,35} Kim *et al.* investigated the comparative photophysical properties of **37c** and **40c**.³⁹ They concluded **40c** increased the overall molecular planarity and rigidity, which explained the relatively long fluorescence lifetimes and red-shifted fluorescence and absorption spectra of **40c**. Tominaga *et al.* also reported the nonplanarity of the macrocycle enhanced the internal conversion from the singlet excited state, which shortened the excited state lifetime of **40c**.⁴⁰

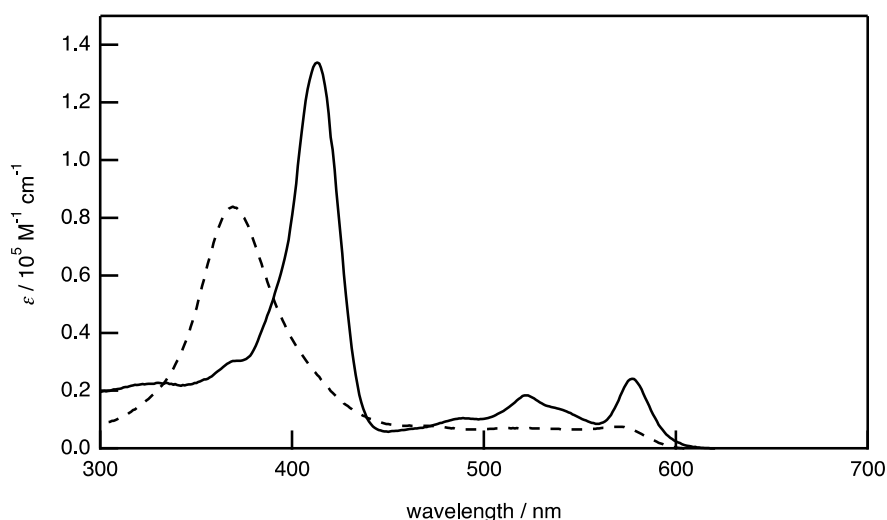
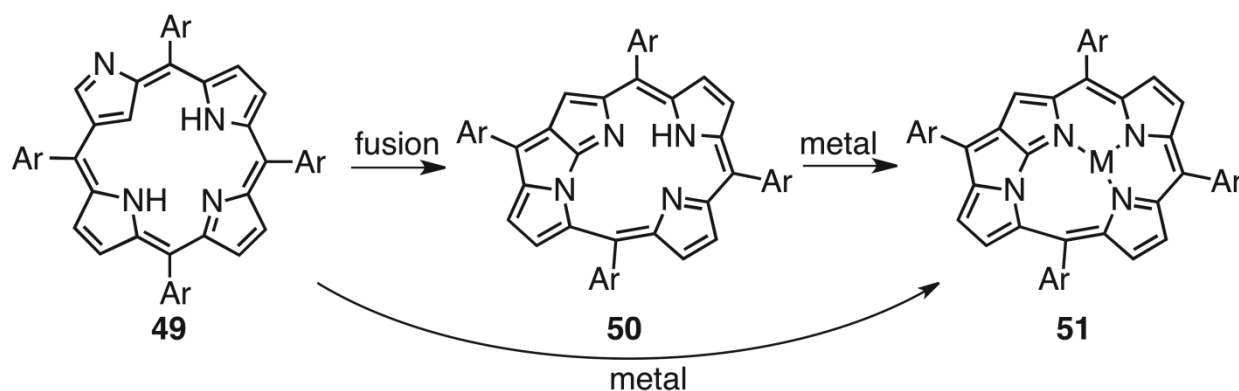


Figure 4. Absorption spectra of **37c** (dotted line) and **40c** (solid line) in CH₂Cl₂

4. SYNTHESIS AND CHARACTERIZATION OF [14]TRIPHYRIN(2.1.1) METAL COMPLEXES

The inner three nitrogen atoms of [14]triphyrin(2.1.1) consist of the two imine and one amine nitrogen atoms and act as monoanionic-tridentate ligands. Cyclic monoanionic tridentate ligands have been extensively studied in the field of coordination-chemistry. The typical examples are subpyrriporphyrin,¹¹ vacataporphyrin,¹³⁻¹⁶ thiaethyneporphyrins,²⁵⁻²⁹ [15]triphyrin(3.1.1)³⁰ and *N*-fused porphyrins (NFPs) (Scheme 16).³⁸ The coordination abilities and properties of their metal complexes except for NFPs have been described above. NFPs **50** also behave as the mono-anionic-tridentate ligands which can coordinate to Re(I),⁴¹ Re(VII),⁴² Mn(I),⁴³ Ru(II),⁴⁴ Fe(II),⁴⁵ B(III),⁴⁶ Si(IV)⁴⁷ and P(V)⁴⁸ ions. These metal complexes have the nature of near-infrared absorption, the generation of singlet oxygen and the ability to work as catalysts. In particular, Re(VII)O₃NFP can catalyze deoxygenation reaction of pyridine *N*-oxide derivatives, affording the corresponding pyridine derivatives quantitatively.⁴² These NFP metal

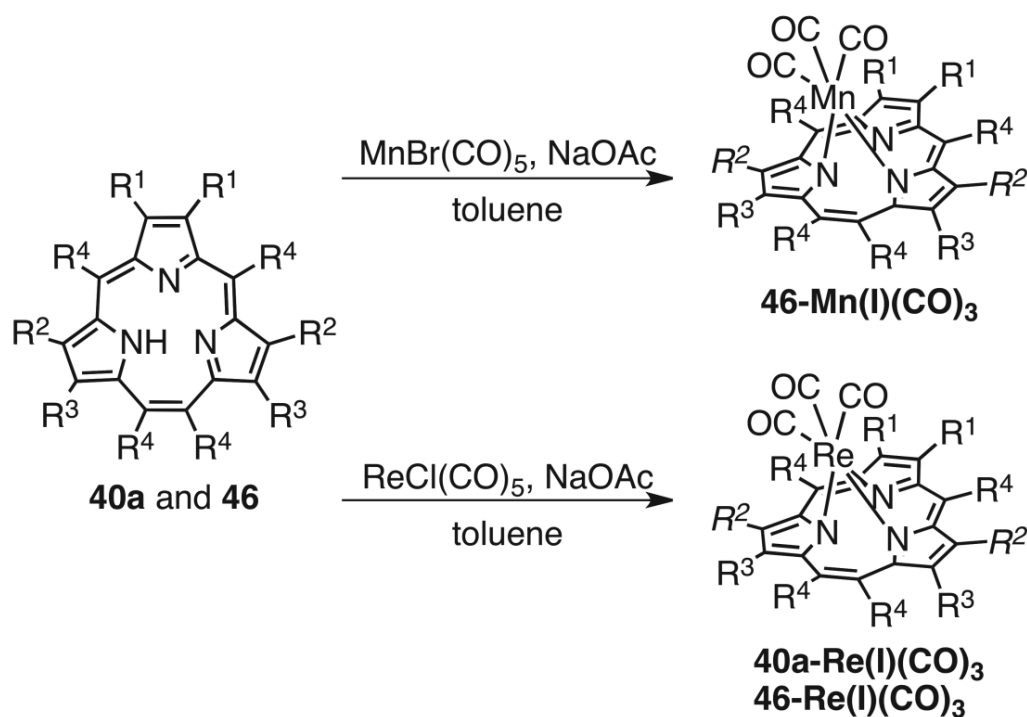
complexes were summarized as good review and book by Furuta.^{44,49} Therefore, in this session we describe the recent results of the metal complexes of [14]triphyrins(2.1.1).



Scheme 16. NFP metal complexes

4-1 OCTAHEDRAL COORDINATED MANGANESE(I), RHENIUM(I) AND RUTHENIUM(II) COMPLEXES

Due to the flexibility of the macrocycle, [14]triphyrin(2.1.1) can coordinate to various metal ions. In 2011, **46-Mn(I)(CO)₃**,³⁴ **46-Re(I)(CO)₃**,³⁴ and **40a-Re(I)(CO)₃**³³ complexes were prepared by the reaction of triphyrins **40a** and **46** with MnBr(CO)₅ or ReCl(CO)₅, in toluene in the presence of NaOAc (Scheme 17).



Scheme 17. Syntheses of triphyrin Mn(I) and Re(I) complexes

The crystal structures are shown in Figure 5. Three inner nitrogen atoms and three CO moieties are coordinated to the Mn(I) or Re(I) ions, respectively. The triphyrins are bowl-shaped structure and Mn and Re ions sit 1.300 Å and 1.455 Å above the plane made by three inner nitrogen atoms, respectively. The distances between C2-C13 and C7-C16 are 5.986(3) and 6.496(3) Å for **46-Mn(I)(CO)₃** and 5.981(3) and 6.383(3) Å for **46-Re(I)(CO)₃**, respectively. The nitrogen-nitrogen distances of N1-N2, N2-N3, and N3-N1 were 2.586(2), 2.594(2), and 2.696(2) Å for **46-Mn(I)(CO)₃** and 2.650(2), 2.654(2), and 2.779(2) Å for **46-Re(I)(CO)₃**, respectively. Each N-N length of **46-Mn(I)(CO)₃** is 0.06 Å shorter than that of **46-Re(I)(CO)₃**, because of the larger size of Re(I) ion than Mn(I) ion. This also influences the shape of the bowl: the curve of **46-Re(I)(CO)₃** is deeper than that of **46-Mn(I)(CO)₃**.

The bowl depth of **40a-Re(I)(CO)₃**, defined as 2.248 Å by the distance from the metal atom to the mean plane of the six peripheral pyrrole β-carbon atoms, is similar to that reported for hydroxy-ligated boron tribenzosubporphyrin (2.33 Å),⁶ but the dihedral angles of the *meso*-aryl substituents (Φ_1 – Φ_4) are significantly larger. The average Re-N and Re-C (CO) bond lengths of 2.129 and 1.915 Å, respectively, are similar to values reported previously for the Re(I)-complex of NFP.⁴¹

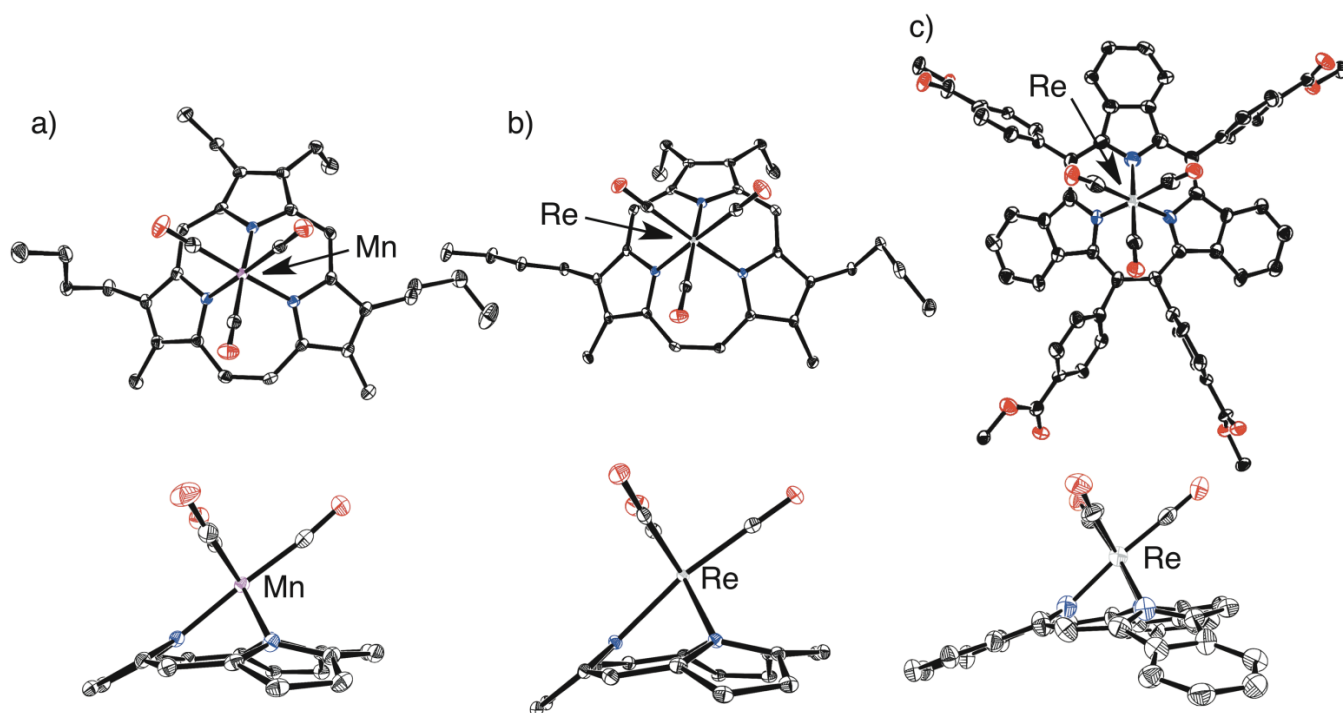
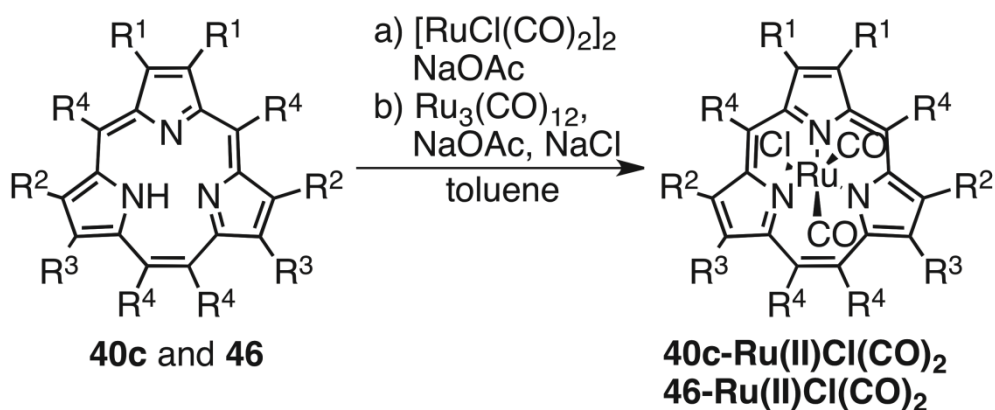


Figure 5. Crystal structures of a) **46-Mn(I)(CO)₃**, b) **46-Re(I)(CO)₃** and c) **40a-Re(I)(CO)₃**. Hydrogen atoms are omitted for clarity. At side view, alkyl chains and aryl group are omitted for clarity. Thermal ellipsoids represent 50% probability.

Ruthenium complex **40c-Ru(II)Cl(CO)₂** was prepared by the reaction of **40c** with Ru₃(CO)₁₂ (Scheme 18).³³ The **40-Ru(II)Cl(CO)₂** and **46-Ru(II)Cl(CO)₂** were also prepared using [Ru(CO)₂Cl]₂.⁵⁰ The X-ray

crystal structure of these Ru(II) complexes were obtained as octahedral structures (Figure 6).



Scheme 18. Synthesis of ruthenium(II) triphyrin complexes

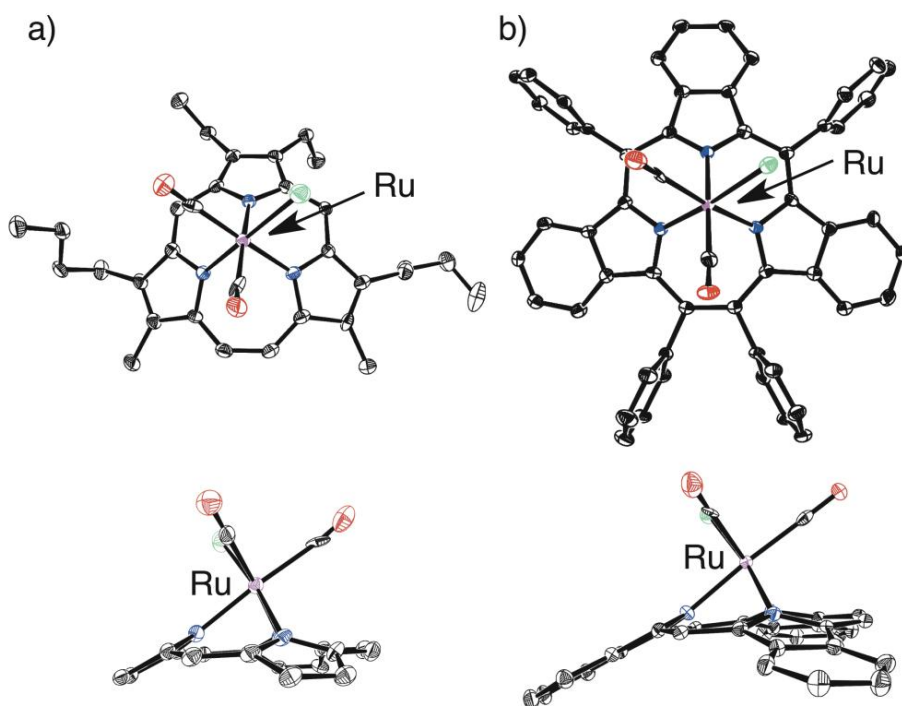
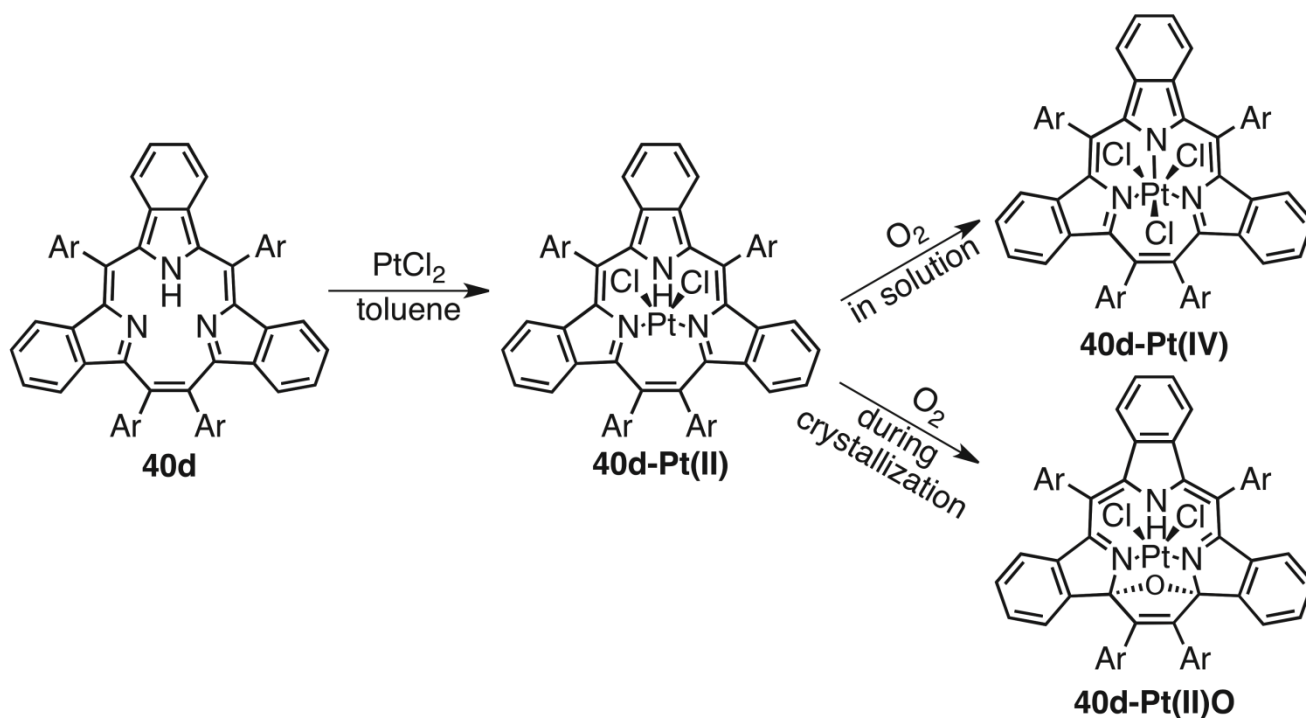


Figure 6. Crystal structures of a) **40-Ru(II)Cl(CO)₂** and b) **46-Ru(II)Cl(CO)₂**. Hydrogen atoms are omitted for clarity. At the side view, alkyl chains and phenyl groups are omitted for clarity. Thermal ellipsoids represent 50% probability.

4-2 PLATINUM(II) AND PLATINUM(IV) COMPLEXES

Considering the tridentate structure of [14]triphyrin(2.1.1), it is challenging to make the square-planar Pt(II) complex. We reported the treatment of **40d** with PtCl₂ under N₂ atmosphere and the subsequent separation over a silica gel column chromatography using CHCl₃ as an eluent to provide **40d-Pt(IV)** as a

green fraction ($R_f = 0.71$) in trace and then **40d-Pt(II)** as a yellow green fraction ($R_f = 0.12$) in 59% yield, respectively (Scheme 19).⁵¹ When the same reaction was performed under air, then **40d-Pt(II)** and **40d-Pt(IV)** were obtained in 47% and 11% yields, respectively. These results suggested the Pt(II) complex was oxidized to Pt(IV) complex under air. The UV-vis spectra of **40d**, **40d-Pt(II)**, and **40d-Pt(IV)** are shown in Figure 7.



Scheme 19. Synthesis and reactivity of platinum(II and IV) triphyrin complexes

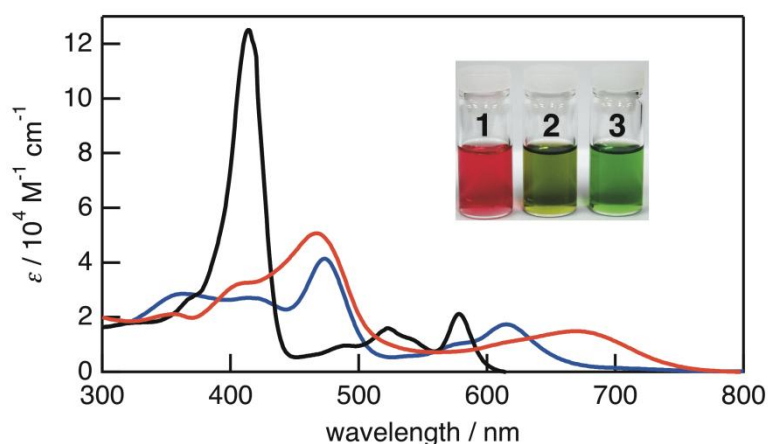


Figure 7. Absorption spectra of free-base triphyrin **40d** (black line), **40d-Pt(II)** (red line) and **40d-Pt(IV)** (blue line) complexes in CH_2Cl_2 . The photograph represents the solution color of 1) **40d**, 2) **40d-Pt(II)** and 3) **40d-Pt(IV)** in CH_2Cl_2 .

Single crystals of **40d-Pt(II)** were obtained from N₂-bubbled solvent (CH₂Cl₂/MeOH) under N₂ atmosphere in a glove box. The crystal structure of **40d-Pt(II)** is shown in Figure 8. The Pt(II) ion is coordinated to two pyrrolic nitrogen atoms and two chloride ions with following bond lengths: 2.021(4) Å for Pt–N(1) and 2.314(1) Å for Pt–Cl in *cis*-configuration to form a rigid square-planar conformation. The triphyrin macrocycle shows saddle shape with C_s symmetry. The mutual angle between two pyrrole rings coordinated to Pt ion is 119.36° with C(1)–C(14) distance of 3.131(7) Å. The angle between the non-coordinated pyrrole ring and the NNCICl plane is 43.69°.

When the **40d-Pt(II)** was crystallized from CH₂Cl₂/EtOH solution under air, green plate-shape crystals were obtained. It was a new Pt(II)-TriP complex, **40d-Pt(II)O**, with oxygen adduct between two pyrrole rings as shown in Figures 8b. The space group of the crystal for **40d-Pt(II)O** was *P2₁/m* and the molecule **40d-Pt(II)O** was positioned in a mirror plane. An oxygen atom is incorporated between C(1) and C(14) atoms to form a 2,5-dihydrofuran ring, with C(1)–O bond length of 1.47(1) Å. The whole molecular π -conjugation system of **40d-Pt(II)O** is interrupted with C(1) sp³ carbons. The bond length of C(15)–C(16) (1.331(1) Å) is close to normal C=C double bond and significantly shorter than that of **40d-Pt(II)** (1.386(7) Å). The bond lengths connected to C(1) atom (1.53(1) Å for C(1)–C(16); 1.52(1) Å for C(1)–C(2); 1.49(1) Å for C(1)–N(1)) in **40d-Pt(II)O** are obviously longer than the corresponding bond lengths of **40d-Pt(II)**, 1.475(19), 1.384(19), and 1.352(6) Å, respectively. The newly formed dihydrofuran moiety shows chair-shape, bended by 33.18° at C(15)–C(16) axis (Figure 8b). The mutual angle between two pyrrole rings coordinated to Pt ion is 109.04° and the C(1)–C(14) distance is only 2.32 Å, indicating the deeper saddle shape compared with **40d-Pt(II)**. The angle between the non-coordinated pyrrole ring and the NNCICl plane of **40d-Pt(II)O** is 46.53°, lifting Pt-plane 2.86° more than **40d-Pt(II)**. The single crystals of **40d-Pt(IV)** were obtained from toluene/*n*-hexane solution. The X-ray structure analysis revealed a bowl-shaped conformation for **40d-Pt(IV)**, similar to **40a-Re(I)(CO)₃**.³³ The distance between Pt(IV) ion and the NNN plane is 1.275 Å, which is shorter than the corresponding distances in Re(I) complex by 0.201 Å and is more flat than the Re(I) complex. The bond length of C(15)–C(16) (1.43(1) Å) is longer than those of **40d-Pt(II)** and **40d-Pt(II)O** and the bond lengths of the macrocyclic ring suggest the clear 14 π -conjugation.

4-3 IRON(II) AND IRON(III) COMPLEXES

Ferrocene, an iron(II) center sandwiched by a pair of aromatic cyclopentadienyl (Cp) ligands, is the first known and archetypal metallocene that was discovered in 1951.⁵² After that, research into ferrocene-containing compounds continues apace within diverse areas.⁵³ However the larger macrocyclic π -conjugated system with monodentate anionic character is little reported so far, due to the weak coordination of π -extended Cp-type ligands. In particular, in porphyrin families there are a few reports in

this context.⁵⁴ (1) Cp-Sc(III)-porphyrin,^{55a} Cp-Zr(II)-porphyrin,^{55b} Cp*-Ru(IV)-porphycene (Cp* = pentamethyl-cyclopentadienyl),⁵⁶ although porphyrin and porphycene are bidentate ligands; (2) β,β' -fused monoruthenocenyloporphyrins and bisferrocenoporphyrins,^{57a} metalporphycenes^{57b} and cyclopentadienylruthenium π complexes of subphthalocyanines^{57c} where five-membered ring part (pyrrole or cyclohexadiene moiety) acted as ligands.⁵⁷ Only recently double-decker iron(II) complexes of

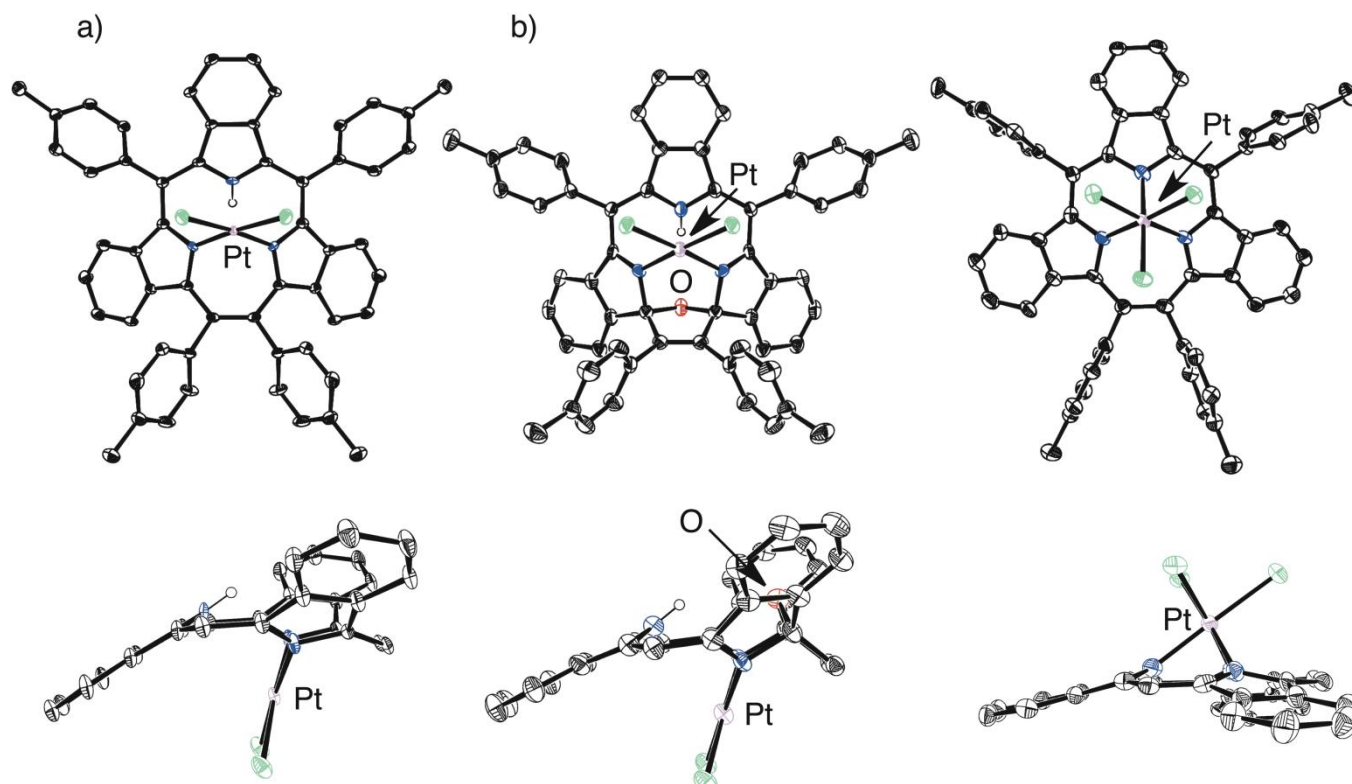


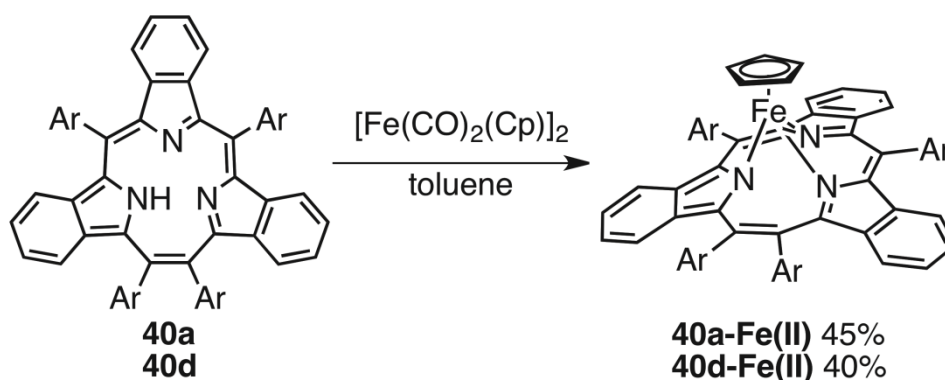
Figure 8. Crystal structures of a) **40d-Pt(II)**, b) **40d-Pt(II)O** and c) **40d-Pt(IV)**. Hydrogen atoms except for inner N-H hydrogen are omitted for clarity. At the side view, aryl groups are omitted for clarity. Thermal ellipsoids represent 50% probability.

dithiaethyneporphyrin²⁶ and NFP,⁴⁵ where macrocycles behaved as macrocyclic tridentate ligands with a single negative charge, have been reported. During the synthesis of NFP complex, the Cp-Fe(II)-NFP has been detected by mass spectra but could not be separated. To date, the synthesis of Cp-Fe(II)-porphyrin sandwich compound remains a considerable challenge.

The treatment of **40a** and **40d** with $[\text{Fe}(\text{CO})_2(\text{Cp})]_2$ gave sandwich η^5 -cyclopentadienyl-iron(II) triphyrin complexes (**40a-Fe(II)** and **40d-Fe(II)**) in 40-45% yields (Scheme 20), whose structures were assigned by ^1H NMR, HR-ESI-MS and X-ray diffraction analysis (Figure 9a).⁵⁸ The redox behavior of Fe ion of the complex was reversible but the potential was 0.54 V lower than that of ferrocene. Fe(III) complex was stable and could be detected by ESR measurement. The protonated Fe(II) complex was easily oxidized to Fe(III) complex to show the same UV-vis spectrum with the electrochemically oxidized Fe(III) complex.

The UV-vis spectrum was reversibly changed to Fe(II) complex by adding DBU.

This stability allowed us to make single crystals of the oxidative state of **40d-Fe(III)**. Fortunately, the crystallization of the oxidized **40d-Fe(II)** with excess amount of $\text{CF}_3\text{SO}_3\text{Ag}$ gave tiny crystals, from which we could perform the X-ray diffraction analysis (Figure 9b). The determined structure contained $[\text{CF}_3\text{SO}_3]_2\text{Ag}^-$ as a counter anion. The Cp ring is coordinated to Fe(III) ion through the five carbon atoms, with the distance of 1.723 Å, which is longer than that of **40d-Fe(II)**, suggesting that the additional positive charge in **40d-Fe(III)** is mostly localized on the formal Fe(III) atom.



Scheme 20. Synthesis of triphyrin iron(II) complexes

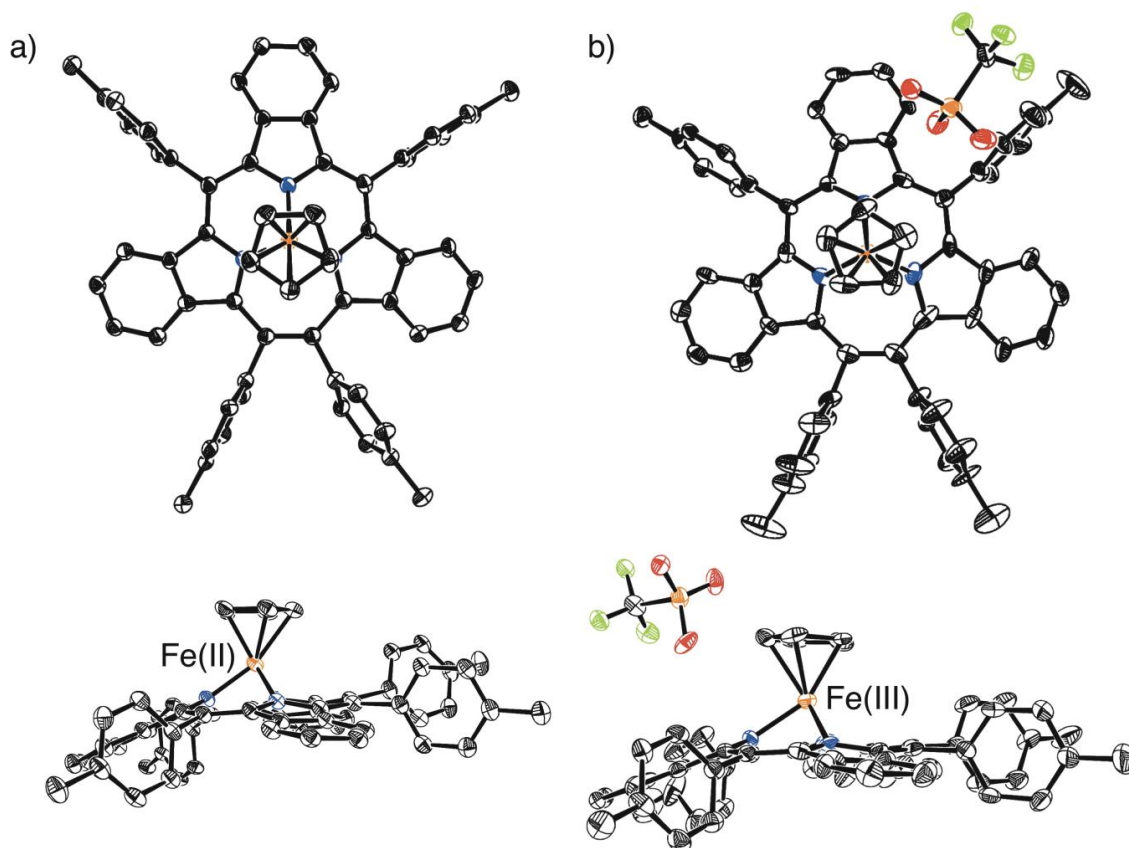
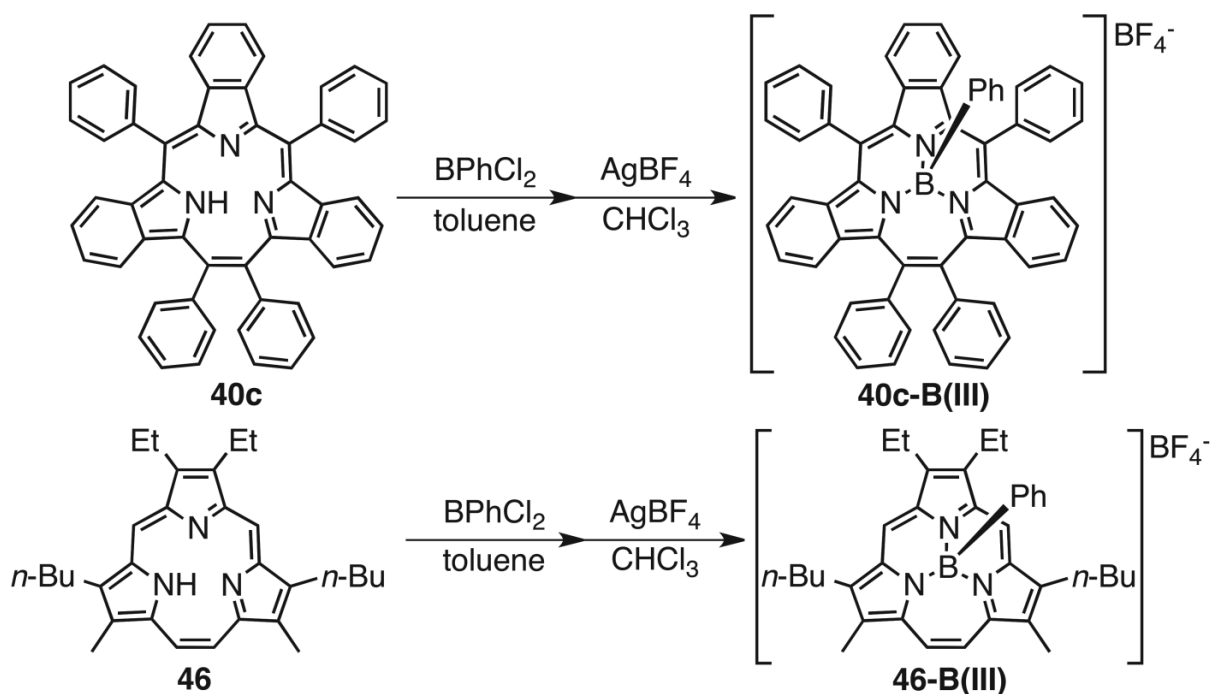


Figure 9. Crystal structures of a) **40d-Fe(II)** and b) **40d-Fe(III)**. Hydrogen atoms are omitted for clarity. At the side view, aryl groups are omitted for clarity. Thermal ellipsoids represent 30% probability.

4-4 TETRAHEDRAL COORDINATED BORON(III) COMPLEXES

The boron complexes of triphyrins are standing on the very important place of the contracted porphyrins since most of the previously reported triphyrins have been coordinated to boron atom. [14]Triphyrins(2.1.1) boron complexes were obtained from free-base [14]triphyrins(2.1.1) **40c** and **46** with phenyl boron dichloride (Scheme 21).⁵⁹ In ¹H NMR spectrum, B-phenyl protons of **46-B(III)** were observed at 3.24 (ortho), 5.99 (meta) and 6.27 (para) ppm, which are the characteristic high-field shifts for the diatropic ring current of the triphyrin macrocycle. The signals of axial phenyl ring of **40c-B(III)** were also observed at 4.00 (ortho), 6.28 (meta) and 6.52 (para) ppm. The crystal structures of **40c-B(III)** and **46-B(III)** are shown in Figure 10. Boron atom was coordinated by three nitrogen atoms and one phenyl carbon atom.



Scheme 21. Synthesis of triphyrin boron(III) complexes

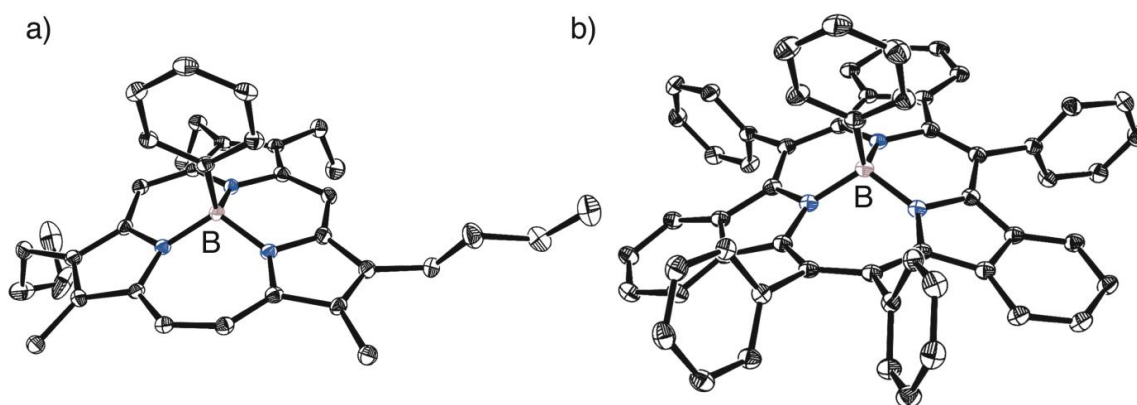


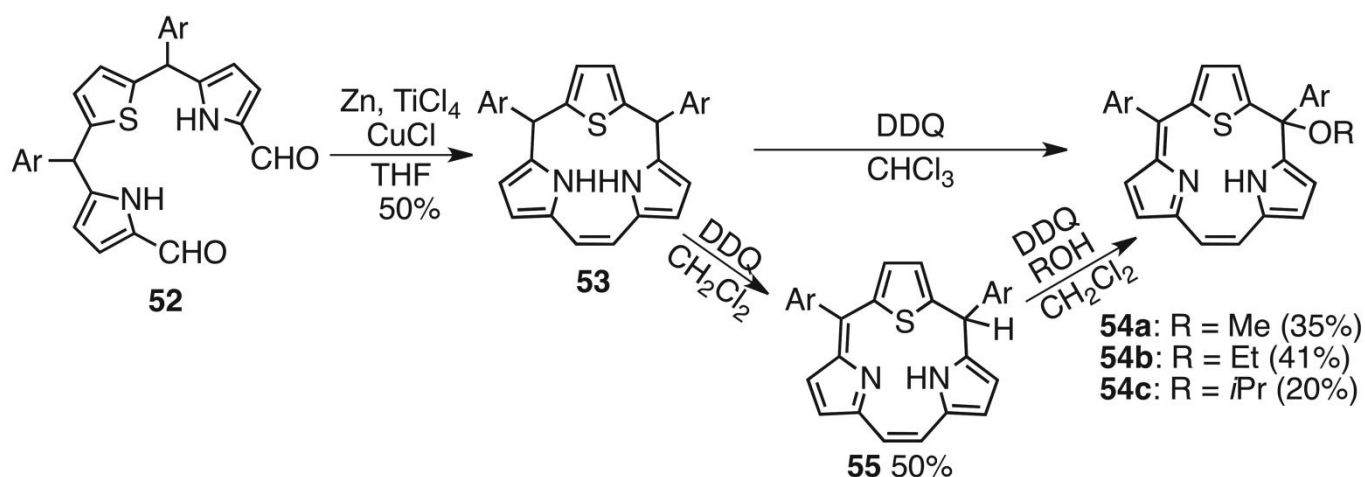
Figure 10. Crystal structures of a) **46-B(III)** and b) **40c-B(III)**. Hydrogen atoms and counter anions are omitted for clarity. Thermal ellipsoids represent 50% probability.

5. CORE-MODIFIED TRIPHRYRINS

5-1 THIATRIPHYRIN(2.1.1) DERIVATIVES

It is well known that remarkable changes in the optical and electrochemical properties and coordination abilities of porphyrins can be induced by core-modification of porphyrinoids.^{60,61} In light of this, it is naturally expected that the core-modification of triphyrins will also give them new functionality.

We tried the McMurry coupling reaction of **52** to give 5,10-dihydro-5,10-ditolylthiatriphyrin **53** in 50% yield, which is an intermediate for the [14]thiatriphyrin(2.1.1) **56** (Scheme 22). The direct oxidation of **53** with 2 eq. of DDQ in CHCl₃ was not successful to give the desired thiatriphyrin **56**, but resulted in the formation of small amount of the thiatriphyrin **54b** with an ethoxy group at the *meso*-position, where ethanol was assumed to come from the presence of ethanol in CHCl₃. The step-wise oxidation of **53** with 1 eq. of DDQ in CH₂Cl₂ gave 5-hydrothiatriphyrin **55** in 50% yield, then the additional oxidation gave the alkoxy-substituted triphyrins **54a-c** in the presence of nucleophile like methanol, ethanol, and isopropanol, respectively. The second oxidation in the absence of nucleophiles induced only the decomposition.⁶²



Scheme 22. Synthetic scheme of alkoxy-substituted thiatriphyrin **54a-c**

Alkoxy group attached thiatriphyrin derivatives **54a-c** were characterized by NMR and X-ray single crystal diffraction analysis. From ¹H NMR, the signal of inner NH-proton of **54b** was observed at 12.7 ppm, which suggested the nature of hydrogen bonds between inner nitrogen atoms. The determined X-ray crystal structure of **54b** is shown in Figure 11a. The ethoxy group is oriented in the same direction as the sulfur atom relative to the plane of the macrocycle. The bond lengths and angles in the pyrrole moieties indicate that one of the pyrrole units has the structure of an imine, whereas the other has an amine structure. This observation suggests a hydrogen-bonding interaction between the two inner nitrogen atoms. The thiophene ring is significantly tilted out of the plane of the macrocycle, with a dihedral angle between the thiophene ring and pyrrole of 69.53°. The elimination of alkoxy groups under acidic

conditions has been performed, following the method reported for subpyrriporphyrins,¹¹ an *N*-fused porphyrin–boron complex,⁴⁶ dithiaethyneporphyrin,²⁵ and a homoporphyrin–nickel complex.⁶³ Then the protonated thiatriphyrin **56**⁺ was obtained by addition of acid and it was reversible to **56** in the presence of DBU (Scheme 23).

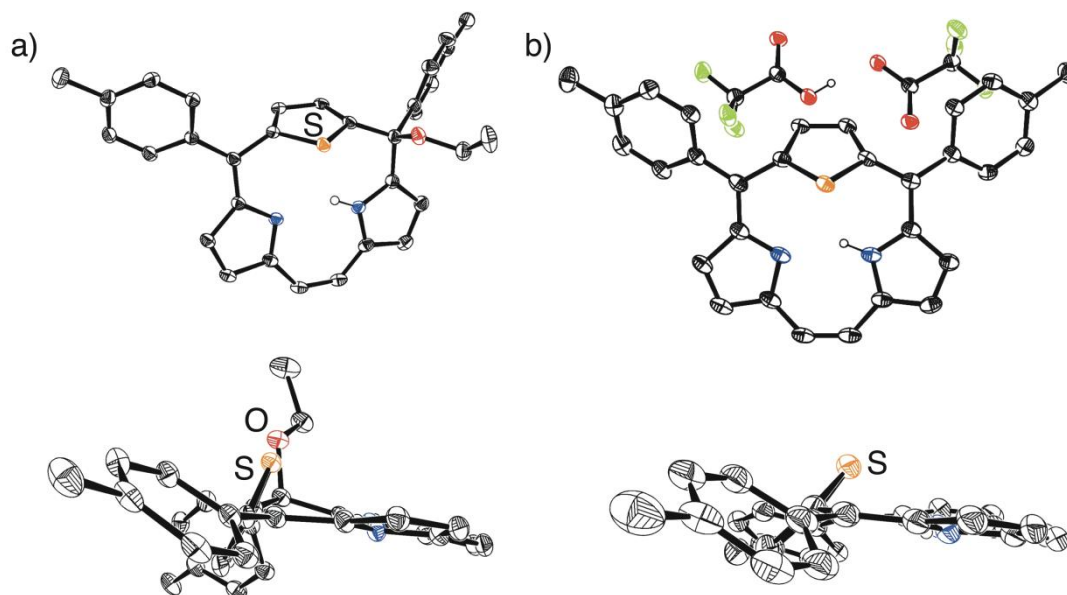
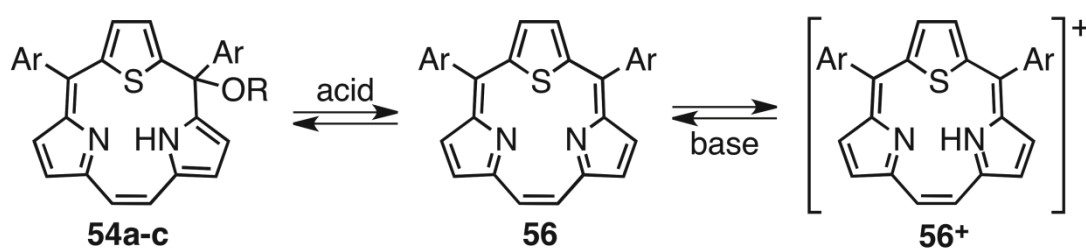


Figure 11. Crystal structures of a) **54b** and b) **56**⁺. Hydrogen atoms expected for inner N–H hydrogen are omitted for clarity. Thermal ellipsoids represent 50% and 30% probabilities for **54b** and **56**⁺, respectively.



Scheme 23. The reactivity of thiatriphyrin derivatives under acid conditions

Fortunately, the crystal structure of **56**⁺ was obtained (Figure 11b). The thiophene ring is also tilted out of the macrocycle plane and the dihedral angle between thiophene ring and pyrrole was 50.28°. Furthermore, the desired thiatriphyrin **56** is expected to have two iminium-type nitrogen and the lone pairs of the nitrogen atoms would be a hindrance to each other to give a stable structure. The protonation of one of the pyrroles would help the stabilization of **56**⁺ by the hydrogen bonding between the two pyrrole rings.

6. CONCLUSION

In this account we have featured on the synthesis, structures and optical properties of a new group of ring-contracted porphyrin, [14]triphyrin(2.1.1) and its metal complexes, in comparison with other ring-contracted porphyrins. [14]Triphyrin(2.1.1) was discovered serendipitously as the first metal-free 14π -porphyrinoid 5 years ago, and afterwards several synthetic routes have been developed by us and others to modify the substituents at *meso*- and β -positions. The remarkable properties of [14]triphyrins(2.1.1) are the flexibility of the macrocycle structure as monoanionic tridentate ligand which enables them to coordinate to a variety of metal ions like Re(I), Mn(I), Ru(II), Pt(II), Pt(IV), Fe(II) and B(III) ions as octahedral, square-planar, sandwich-type or tetrahedral complexes. Core-modified triphyrins might be also realizable considering the synthetic scheme, but thiatriphyrin was not isolated due to the large atomic diameter of sulfur atom in the triphyrin cavity and the electronic repulsion of lone pairs of inner nitrogen atoms, instead alcohol adducts were obtained successfully. Further synthesis of metal complexes and core-modified triphyrins will be possible and various properties and functions are remains to be found.

ACKNOWLEDGEMENTS

This work was partly supported by JSPS Postdoctoral Fellowship for Foreign Researchers, Grants-in-Aid No 24655034 and the Green Photonics Project in NAIST sponsored by the MEXT, Japan. We thank Prof. Hidemitsu Uno and Dr. Shigeki Mori in Ehime University and Prof. Naoki Aratani in Nara Institute of Science and Technology for the X-ray single crystal analysis of [14]triphyrin(2.1.1) compounds. Finally, special thanks are given to those listed as the coauthors in our papers cited here, particularly to Dr. Zhao-Li Xue in Jiangsu University, Prof. Zhen Shen in Nanjing University and Yuka Sakakibara in NAIST for their contribution to these results.

REFERENCES (AND NOTES)

1. For reviews. a) Z. Gross, *J. Biol. Inorg. Chem.*, 2001, **6**, 733; b) D. T. Gryko, *Eur. J. Org. Chem.*, 2002, 1735; c) A. Ghosh and E. Steene, *J. Inorg. Biochem.*, 2002, **91**, 423; d) I. Aviv and Z. Gross, *Chem. Commun.*, 2007, 1987; e) L. Flamigni and D. T. Gryko, *Chem. Soc. Rev.*, 2009, **38**, 1635; f) I. Aviv-Harel and Z. Gross, *Chem. Eur. J.*, 2009, **15**, 8382; g) H.-Y. Liu, M. H. R. Mahmood, S.-X. Qiu, and C. K. Chang, *Coord. Chem. Rev.*, 2013, **257**, 1306.
2. a) A. Ghosh, I. H. Wasbotten, W. Davis, and J. C. Swarts, *Eur. J. Inorg. Chem.*, 2005, 4479; b) M. Bröring, S. Köhler, and C. Kleeberg, *Angew. Chem. Int. Ed.*, 2008, **47**, 5658; c) T. Ito, Y. Hayashi, S. Shimizu, J.-Y. Shin, N. Kobayashi, and H. Shinokubo, *Angew. Chem. Int. Ed.*, 2012, **51**, 8542.
3. For reviews. a) A. Jasat and D. Dolphin, *Chem. Rev.*, 1997, **97**, 2267; b) J. L. Sessler and D. Seidel,

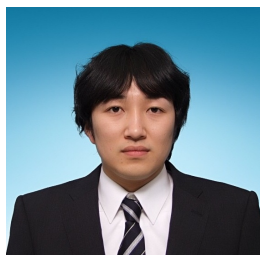
- [Angew. Chem. Int. Ed.](#), 2003, **42**, 5134; c) J. M. Lim, Z. S. Yoon, J.-Y. Shin, K. S. Kim, M.-C. Yoon, and D. Kim, [Chem. Commun.](#), 2009, 261; d) S. Saito and A. Osuka, [Angew. Chem. Int. Ed.](#), 2011, **50**, 4342; e) M. Stępień, N. Sprutta, and L. Latos-Grażyński, [Angew. Chem. Int. Ed.](#), 2011, **50**, 4288.
4. A. Meller and A. Ossko, [Monatsh. Chem.](#), 1972, **103**, 150.
 5. M. S. Rodríguez-Morgade, S. Esperanza, T. Torres, and J. Barberá, [Chem. Eur. J.](#), 2005, **11**, 354.
 6. Y. Inokuma, J. H. Kwon, T. K. Ahn, M.-C. Yoo, D. Kim, and A. Osuka, [Angew. Chem. Int. Ed.](#), 2006, **45**, 961.
 7. Y. Inokuma, Z. S. Yoon, D. Kim, and A. Osuka, [J. Am. Chem. Soc.](#), 2007, **129**, 4747.
 8. N. Kobayashi, Y. Takeuchi, and A. Matsuda, [Angew. Chem. Int. Ed.](#), 2007, **46**, 758.
 9. E. Tsurumaki, S. Hayashi, F. S. Tham, C. A. Reed, and A. Osuka, [J. Am. Chem. Soc.](#), 2011, **133**, 11956.
 10. a) C. G. Claessens, D. González-Rodríguez, and T. Torres, [Chem. Rev.](#), 2002, **102**, 835; b) Y. Inokuma and A. Osuka, [Dalton Trans.](#), 2008, 2517; c) A. Osuka, E. Tsurumaki, and T. Tanaka, [Bull. Chem. Soc. Jpn.](#), 2011, **84**, 679.
 11. R. Myśliborski, L. Latos-Grażyński, L. Szterenber, and T. Lis, [Angew. Chem. Int. Ed.](#), 2006, **45**, 3670.
 12. K. S. Kim, J. M. Lim, R. Myśliborski, M. Pawlicki, L. Latos-Grażyński, and D. Kim, [J. Phys. Chem. Lett.](#), 2011, **2**, 477.
 13. E. Pacholska, L. Latos-Grażyński, and Z. Ciunik, [Chem. Eur. J.](#), 2002, **8**, 5403.
 14. E. Pacholska-Dudziak, J. Skonieczny, M. Pawlicki, L. Szterenber, and L. Latos-Grażyński, [Inorg. Chem.](#), 2005, **44**, 8794.
 15. E. Pacholska-Dudziak, A. Gaworek, and L. Latos-Grażyński, [Inorg. Chem.](#), 2011, **50**, 10956.
 16. E. Pacholska-Dudziak, J. Skonieczny, M. Pawlicki, L. Szterenber, Z. Ciunik, and L. Latos-Grażyński, [J. Am. Chem. Soc.](#), 2008, **130**, 6182.
 17. T. D. Lash, S. A. Jones, and G. M. Ferrence, [J. Am. Chem. Soc.](#), 2010, **132**, 12786.
 18. E. Pacholska-Dudziak, L. Szterenber, and L. Latos-Grażyński, [Chem. Eur. J.](#), 2011, **17**, 3500.
 19. M. Klyta, P. Ostasiewicz, K. Jurczyszyn, K. Duś, L. Latos-Grażyński, E. Pacholska-Dudziak, and P. Ziółkowski, [Laser Surg. Med.](#), 2011, **43**, 607.
 20. J. L. Sessler, T. Murai, V. Lynch, and M. Cyr, [J. Am. Chem. Soc.](#), 1988, **110**, 5586.
 21. a) J. L. Sessler, G. Hemmi, T. D. Mody, T. Murai, A. Burrell, and S. W. Young, [Acc. Chem. Res.](#), 1994, **27**, 43; b) J. L. Sessler, V. Král, M. C. Hoehner, K. O. A. Chin, and R. M. Dávila, [Pure Appl. Chem.](#), 1996, **68**, 1291; c) J. L. Sessler and R. A. Miller, [Biochem. Pharmacol.](#), 2000, **59**, 733; d) D. J. Magda, Z. Wang, N. Gerasimchuk, W. Wei, P. Anzenbacher, and J. L. Sessler, [Pure Appl. Chem.](#), 2004, **76**, 365; e) S. R. Thomas and D. Khuntia, [Int. J. Nanomedicine](#), 2007, **2**, 79; f) J. F. Arambula,

- C. Preihs, D. Borthwick, D. Magda, and J. L. Sessler, *Anticancer Agents Med. Chem.*, 2011, **11**, 222;
- g) C. Preihs, J. F. Arabula, D. Magda, H. Jeong, D. Yoo, J. Cheon, Z. H. Siddik, and J. L. Sessler, *Inorg. Chem., Article ASAP*, DOI: [10.1021/ic400226g](https://doi.org/10.1021/ic400226g).
22. 'Expanded. Contracted & Isomeric Porphyrins', J. L. Sessler and D. T. Gryko, Pergamon, 1997.
23. C. H. Lee, J. W. Ka, and D. H. Won, *Tetrahedron Lett.*, 1999, **40**, 6799.
24. C. H. Lee and K. T. Oh, *Tetrahedron Lett.*, 1999, **40**, 1921.
25. A. Berlicka, L. Latos-Grażyński, and T. Lis, *Angew. Chem. Int. Ed.*, 2005, **44**, 5288.
26. A. Berlicka and L. Latos-Grażyński, *Inorg. Chem.*, 2009, **48**, 7922.
27. A. Berlicka, L. Latos-Grażyński, L. Szterenberga, and M. Pawlicki, *Eur. J. Org. Chem.*, 2010, 5688.
28. A. Berlicka, N. Sprutta, and L. Latos-Grażyński, *Chem. Commun.*, 2006, 3346.
29. E. Nojman, A. Berlicka, L. Szterenberga, and L. Latos-Grażyński, *Inorg. Chem.*, 2012, **51**, 3247.
30. A. Krivokapic, A. R. Cowley, and H. L. Anderson, *J. Org. Chem.*, 2003, **68**, 1089.
31. Z.-L. Xue, Z. Shen, J. Mack, D. Kuzuhara, H. Yamada, T. Okujima, N. Ono, X.-Z. You, and N. Kobayashi, *J. Am. Chem. Soc.*, 2008, **130**, 16478.
32. S. Ito, T. Murashima, N. Ono, and H. Uno, *Chem. Commun.*, 1998, 1661.
33. Z.-L. Xue, J. Mack, H. Lu, L. Zhang, X.-Z. You, D. Kuzuhara, M. Stillman, H. Yamada, S. Yamauchi, N. Kobayashi, and Z. Shen, *Chem. Eur. J.*, 2011, **17**, 4396.
34. D. Kuzuhara, H. Yamada, Z.-L. Xue, T. Okujima, S. Mori, Z. Shen, and H. Uno, *Chem. Commun.*, 2011, **47**, 722.
35. K. S. Anju, S. Ramakrishnan, and A. Srinivasan, *Org. Lett.*, 2011, **13**, 2498.
36. E. Vogel, M. Köcher, H. Schmickler, and J. Lex, *Angew. Chem., Int. Ed. Engl.*, 1986, **25**, 257.
37. E. Vogel, B. Binsack, Y. Hellwig, C. Erben, A. Heger, J. Lex, and Y.-D. Wu, *Angew. Chem., Int. Ed. Engl.*, 1997, **36**, 2612.
38. H. Furuta, T. Ishizuka, A. Osuka, and T. Ogawa, *J. Am. Chem. Soc.*, 1999, **121**, 2945.
39. Y. M. Sung, J. M. Lim, Z.-L. Xue, Z. Shen, and D. Kim, *Chem. Commun.*, 2011, **47**, 12616.
40. Y. Iima, D. Kuzuhara, Z.-L. Xue, H. Uno, S. Akimoto, H. Yamada, and K. Tominaga, *Chem. Phys. Lett.*, 2011, **513**, 67.
41. a) M. Toganoh, T. Ishizuka, and H. Furuta, *Chem Commun.*, 2004, 2464; b) M. Toganoh, S. Ikeda, and H. Furuta, *Inorg. Chem.*, 2007, **46**, 10003.
42. M. Toganoh, S. Ikeda, and H. Furuta, *Chem. Commun.*, 2005, 4589.
43. S. Ikeda, M. Toganoh, and H. Furuta, *Inorg. Chem.*, 2011, **50**, 6029.
44. M. Toganoh and H. Furuta, *Handbook of Porphyrin Science*, ed. by K. M. Kadish, K. M. Smith, and R. Guilard, *World Scientific Publication Co. Pte. Ltd., Singapore*, 2010, Vol. 2, pp. 295-367.
45. M. Toganoh, A. Sato, and H. Furuta, *Angew. Chem. Int. Ed.*, 2011, **50**, 2752.

46. A. Młodzianowska, L. Latos-Grażyński, L. Szterenber, and M. Stępień, [Inorg. Chem., 2007, 46, 6950](#).
47. J. Skonieczny, L. Latos-Grażyński, and L. Szterenber, [Inorg. Chem., 2009, 48, 7394](#).
48. A. Młodzianowska, L. Latos-Grażyński, and L. Szterenber, [Inorg. Chem., 2008, 47, 6364](#).
49. M. Toganoh and H. Furuta, [Chem. Commun., 2012, 48, 937](#).
50. Unpublished data.
51. Z.-L. Xue, D. Kuzuhara, S. Ikeda, T. Okujima, S. Mori, H. Uno, and H. Yamada, [Inorg. Chem., 2013, 52, 1688](#).
52. a) T. J. Kealy and P. L. Pauson, [Nature, 1951, 168, 1039](#); b) *Ferrocenes: Ligands, Materials and Biomolecules* (Ed. by P. Stepnicka), Wiley, Chichester, 2008.
53. C. Bucher, C. H. Devillers, J.-C. Moutet, G. Royal, and E. Saint-Aman, [Coord. Chem. Rev., 2009, 253, 21](#).
54. L. Cuesta, J. L. Sessler, [Chem. Soc. Rev., 2009, 38, 2716](#) and references cited therein.
55. a) J. Arnold and G. C. Hoffman, [J. Am. Chem. Soc., 1990, 112, 8620](#); b) H.-J. Kim, S. Jung, Y.-M. Jeon, D. Whang, and K. Kim, [Chem. Commun., 1997, 2201](#).
56. L. Cuesta, E. Karnas, V. M. Lynch, P. Chen, J. Shen, K. M. Kadish, K. Ohkubo, S. Fukuzumi, and J. L. Sessler, [J. Am. Chem. Soc., 2009, 131, 13538](#).
57. a) H. J. H. Wang, L. Jaquinod, M. M. Olmstead, M. G. H. Vicente, K. M. Kadish, Z. Ou, and K. M. Smith, [Inorg. Chem., 2007, 46, 2898](#); b) G. I. Vargas-Zúñiga, V. V. Roznyatovskiy, A. Nepomnyaschii, V. M. Lynch, and J. L. Sessler, [J. Porphyrins Phthalocyanines, 2012, 16, 479](#); c) E. Caballero, J. Fernández-Ariza, V. M. Lynch, C. Romero-Nieto, M. S. Rodríguez-Morgade, J. L. Sessler, D. M. Guldi, and T. Torres, [Angew. Chem. Int. Ed., 2012, 51, 11337](#).
58. Z. Xue, D. Kuzuhara, S. Ikeda, Y. Sakakibara, K. Ohkubo, N. Aratani, T. Okujima, H. Uno, S. Fukuzumi, and H. Yamada, *Angew. Chem. Int. Ed.*, DOI: 10.1002/anie.201302815 and 10.1002/ange.201302815.
59. D. Kuzuhara, Z. Xue, S. Mori, T. Okujima, H. Uno, and H. Yamada, *Chem. Commun.*, to be submitted.
60. L. Latos-Grażyński in *The Porphyrin Handbook Vol. 2*, (Ed. by K. M. Kadish, K. M. Smith, and R. Guilard), Academic Press, San Diego, 2000, pp. 361-416.
61. P. J. Chmielewski and L. Latos-Grażyński, [Coordin. Chem. Rev., 2005, 249, 2510](#).
62. D. Kuzuhara, Y. Sakakibara, S. Mori, T. Okujima, H. Uno, and H. Yamada, [Angew. Chem. Int. Ed., 2013, 52, 3360](#).
63. H. J. Callot and E. Schaeffer, [J. Org. Chem., 1977, 42, 1567](#).



Dr. Hiroko Yamada was born in Kamakura. She received her Ph.D. degree in 1992 from Kyoto University, under the guidance of Prof. Kazuhiro Maruyama and Prof. Atsuhiro Osuka. She was selected as a Research Fellow of the Japan Society for the Promotion of Science (JSPS) in 1992-1994. In 1993, she did her research in Argonne National Laboratory, USA. In 1994, she joined International Research Laboratory, Ciba-Geigy Ltd., then moved to Ciba Specialty Chemicals Inc. She started her academic career in 1998 as a post-doctorate researcher at the Institute of Scientific and Industrial Research (ISIR), Osaka University, then a post-doctorate researcher of CREST, JST at Graduate School of Engineering, Osaka University. Since 2003, she was an associate professor in Graduate School of Science and Engineering, Ehime University, and moved to an associate professor in Graduate School of Materials Science, Nara Institute of Science and Technology in 2011. She was promoted to a full professor in 2012. In 2006–2010, she was a researcher of PRESTO, JST, and from 2010 a group leader of CREST project, JST. Awards: Incentive Award of Chugoku-Shikoku Branch, The Society of Synthetic Organic Chemistry (2009), The Maruyama Memorial Research Award (2010), The Japanese Photochemistry Association Award (2012).



Dr. Daiki Kuzuhara was born in 1983 in Ehime, Japan. He received his PhD from Ehime University under the supervision of Prof. Hiroko Yamada. He was selected as a Research Fellow of the Japan Society for the Promotion of Science for young scientists in 2010. He is now an assistant professor at Graduate School of Materials Science, Nara Institute of Science and Technology. His current research interests are focused on the synthesis of the various porphyrinoids including the ring contracted-porphyrins and the functional organic materials for organic electronics.